Selection of Vibrio crassostreae relies on a plasmid expressing a type 6 secretion system cytotoxic for host immune cells

Damien Piel, Maxime Bruto, Adèle James, Yannick Labreuche, Christophe Lambert, Adrian Janicot, Sabine Chenivesse, Bruno Petton, K Mathias Wegner, Candice Stoudmann, et al.

Title: Selection of *Vibrio crassostreae* relies on a plasmid expressing a type 6 secretion system cytotoxic for host immune cells

Damien Piel[1,2*], Maxime Bruto[2*], Adèle James[1,2*], Yannick Labreuche[1,2], Christophe Lambert[3], Adrian Janicot[2], Sabine Chenivesse[2], Bruno Petton[1,3], K. Mathias Wegner[4], Candice Stoudmann[5], Melanie Blokesch[5] and Frédérique Le Roux[1,2#]

Running Head: *V. crassostreae* cytotoxicity relies on a T6SS

[1]Ifremer, Unité Physiologie Fonctionnelle des Organismes Marins, ZI de la Pointe du Diable, CS 10070, F-29280 Plouzané, France

[2]Sorbonne Universités, UPMC Paris 06, CNRS, UMR 8227, Integrative Biology of Marine Models, Station Biologique de Roscoff, CS 90074, F-29688 Roscoff cedex, France

[3]Laboratoire des Sciences de l'Environnement Marin (LEMAR), UMR 6539 CNRS UBO IRD IFREMER – Institut Universitaire Européen de la Mer, Technopôle Brest-Iroise – Rue Dumont d'Urville, F-29280 Plouzané, France

[4]AWI - Alfred Wegener Institut - Helmholtz-Zentrum für Polar- und Meeresforschung, Coastal Ecology, Waddensea Station Sylt, Hafenstrasse 43, 25992 List, Germany

[5]Laboratory of Molecular Microbiology, Global Health Institute, School of Life Sciences, Ecole Polytechnique Fédérale de Lausanne (EPFL), CH-1015 Lausanne, Switzerland

[*]These authors contribute equally to this work.

[#]**Corresponding author:** Frédérique Le Roux

Equipe Génomique des Vibrios, UMR 8227, Integrative Biology of Marine Models, Station Biologique de Roscoff, CS 90074, F-29688, Roscoff cedex, France

Tel: 33 2 98 29 56 47, frederique.le-roux@sb-roscoff.fr

ORIGINALITY-SIGNIFICANCE STATEMENT

A recent study highlighted the role of a herpes virus as primary etiological agent of Pacific oyster mortality syndrome (POMS), which affects juveniles of the oyster *Crassostrea gigas*. We show here that the selection of virulent bacteria in oyster farms is also an important piece of the POMS puzzle. This bacteria taxonomically assigned to *Vibrio crassostreae* species, carries a plasmid that encodes a Type 6 Secretion System (T6SS), which increases its ability to kill the major cellular players of oyster immunity, the hemocytes. This T6SS was identified in two additional species that infect mollusks, suggesting a parallel evolution of these pathogens. Finally, our results indicate that broad range of pathogens kill their hosts via hemocyte cytotoxicity.

ABSTRACT

Pacific oyster mortality syndrome affects juveniles of *Crassostrea gigas* oysters and threatens the sustainability of commercial and natural stocks of this species. *Vibrio crassostreae* has been repeatedly isolated from diseased animals and the majority of the strains have been demonstrated to be virulent for oysters. In this study we showed that oyster farms exhibited a high prevalence of a virulence plasmid carried by *V. crassostreae* while oysters, at an adult stage, were reservoirs of this virulent population. The pathogenicity of *V. crassostreae* depends on a novel transcriptional regulator, which activates the bidirectional promoter of a Type 6 Secretion System (T6SS) genes cluster. Both the T6SS and a second chromosomal virulence factor, *r5.7*, are necessary for virulence but act independently to cause to hemocyte (oyster immune cell) cytotoxicity. A phylogenetically closely related T6SS was identified in *V. aestuarianus* and *V. tapetis*, which infect adult oysters and clams, respectively. We propose that hemocyte cytotoxicity, is a lethality trait shared by a broad range of mollusk pathogens and we speculate that T6SS was involved in parallel evolution of pathogen for mollusks.

INTRODUCTION

The Pacific oyster mortality syndrome (POMS) affects juveniles of *Crassostrea gigas*, the main oyster species exploited worldwide. This syndrome occurs when the seawater temperature reaches 16°C and is caused by multiple infections with an initial and necessary step relying on infection of the hemocytes, the oyster immune cells, by the endemic Ostreid herpesvirus OsHV-1 µVar (de Lorgeril et al., 2018). Viral replication leads to the host entering an immune-compromised state, evolving towards subsequent bacteremia involving opportunistic bacteria such as *Vibrio sp.* Exploring POMS in an oyster farming area from the French North Atlantic cost (Brest), we showed previously that the onset of disease is associated with progressive replacement of diverse benign colonizers by members of a phylogenetically coherent virulent population, *V. crassostreae* (Lemire et al., 2015). The virulent population is genetically diverse but most members of the population can cause disease. We further demonstrated that *V. crassostreae* virulence depends on the presence of a large mobilizable plasmid, pGV1512 (hereafter named pGV for simplicity) although the mechanisms underpinning virulence remain to be elucidated (Bruto et al., 2017). Having observed that juvenile infection by *V. crassostreae* is recurrent in the POMS occurring in Brest (Bruto et al., 2017, de Lorgeril et al., 2018, Lemire et al., 2015), the questions arose whether oyster farms create conditions that lead to the selection of this virulence plasmid and whether oysters (farmed or wild) represent a reservoir of virulent *V. crassostreae*. Indeed, it has been suggested that, during cold months, oysters act as a reservoir for *V. aestuarianus* (Goudenege et al., 2015, Parizadeh et al., 2018), a pathogen that primarily targets adult animals and hence is not thought to be involved in POMS (Azema et al., 2017).

Pathogenic lifestyles are typically associated with horizontal acquisition of virulence genes (Le Roux and Blokesch, 2018), but pre-existing genomic features might be necessary for the acquisition and/or the functionality of these virulence genes (Shapiro et al., 2016). Indeed, we showed that a core gene, *r5.7*, which encodes an exported protein of unknown function, is necessary for full virulence in *V. crassostreae* (Lemire et al., 2015). This gene is widely distributed across the Splendidus clade, a large group of closely-related species (*e.g., V. splendidus, V. crassostreae, V. cyclitrophicus).* The *r5.7* gene was acquired by the common ancestor of this group and co-diversified in some populations while being lost from non-virulent populations (Bruto et al., 2018). The widespread occurrence of *r5.7* across environmental *Vibrio* populations suggests that it has an important biological role but its frequency also indicates that this role is population-specific. Indeed, it was recently showed that *r5.7* is involved in population-specific mechanisms of hemocyte cytotoxicity (Rubio et al., in press). In *V. crassostreae* hemocyte cytotoxicity is contact-dependent and requires *r5.7.* The R5.7 protein is not lethal when injected into oysters, but this protein is able to restore virulence when co-injected with a mutant lacking the *r5.7* gene (Bruto et al., 2018). This suggests that R5.7 interacts with the external surface of *Vibrio* and / or with a cellular target. Whether *r5.7* and the virulence gene(s) encoded by the pGV plasmid act in concert or independently to promote *V. crassostreae* virulence and cytotoxicity was a goal of this study.

Here, we explored the distribution and functional interaction of two *V. crassostreae* virulence determinants, R5-7 and the plasmid pGV. *V. crassostreae* strains were collected from Brest (France), an area of intense oyster farming that is experiencing recurrent mortality events, and in Sylt (Germany) where a massive oyster invasion formed natural beds that have not yet suffered from *Vibrio*-related disease outbreaks (Reise et al., 2017). While the *r5.7* gene was detected at

high frequency in *V. crassostreae*, the pGV plasmid was detected only in isolates from Brest and its presence correlated with virulence as assessed by experimental oyster infections. We further showed that, at a temperature of <16°C, oysters act as a reservoir of *V. crassostreae* strains. Exploring genetically the virulence determinants carried by the plasmid we showed that a transcriptional regulator is necessary for pGV-mediated virulence. This regulator induces the expression of a molecular killing device called the type 6 secretion system (T6SS) which is also necessary for full virulence. RNA sequencing (RNAseq) followed by transcriptional fusion analysis led us to identify a bidirectional promoter within the T6SS genes cluster that is up-regulated by the transcriptional activator. Gene deletions and complementation experiments further confirmed the role of the *r5.7* and the T6SS in hemocyte cytotoxicity and indicated that they act in an additive manner. Finally, the identification of a similar type of T6SS in *V. aestuarianus* and *V. tapetis* led us to hypothesis a parallel evolution of mollusk pathogens.

RESULTS

The virulence plasmid is widespread in *V. crassostreae* population occurring in oyster farms

We previously hypothesized that the introgression of the virulence plasmid pGV into *V. crassostreae* might have been favored by elevated host density in farming areas (Bruto et al., 2017). However, wild oyster beds can also reach high densities, as exemplified by the recent invasion of *C. gigas* oysters into the Wadden sea (North Sea) (Reise et al., 2017). To date, no *Vibrio*-associated mass mortalities have been observed in this area, in contrast to observations in heavily farmed areas. We thus investigated the presence and frequency of the pGV plasmid in *V. crassostreae* strains sampled from Sylt. For this, 910 *Vibrio* strains were isolated from

seawater fractions and oysters from Sylt, genotyped by partial *hsp60* gene sequencing and assigned to *Vibrio* populations as described previously (Figure S1). Multi Locus Sequencing Typing (MLST) further confirmed the taxonomic assignment of 47 *V. crassostreae* strains isolated from Sylt (Figure 1, beige squares) as well as 42 isolates from Brest (Figure 1, brown squares) (Table S1). The phylogenetic structure partitioned these strains into two clades representing the two locations. The first clade contained the majority of strains from Sylt (68%, 32 out of 47), while the second clade principally contained strains from Brest (80%, 34 out of 42). The pGV *repB* gene was never detected in isolates from Sylt and was mainly detected in strains from Brest that belonged to clade 2 (Figure 1, plain blue circles). Only one clade 1 strain (8T5_11), originating from Brest, was found to be positive for *repB*. The presence of the plasmid was confirmed by sequencing the genome of the 8T5_11 strain (Table S2). We next explored the virulence of these isolates by experimental infection. When the 47 and 42 *V. crassostreae* strains isolated from Sylt and Brest, respectively, were injected individually into oysters, we observed that virulence was strongly correlated with the presence of the plasmid (50 to 100% oyster mortalities, 24 hours post injection), supporting previous findings (Bruto et al., 2017). Only three strains carrying the plasmid (8T5_11, 7T7_10 and 8T7_10) induce a weak mortality (<20%) (Figure 1). Gene loss could explain this non-virulent phenotype. Indeed, comparative genomic analyses identified 44 genes that were absent from the 8T5_11 genome but were present in all of the sequenced virulent strains of *V. crassostreae* (Figure 1; Table S3). These 44 genes included *r5.7*, which is necessary for virulence and is located in a region that was previously identified as being specific to *V. crassostreae* (Lemire et al., 2015). However the expression of *r5.7* from a plasmid had no effect on 8T5_11 virulence (Figure S2). Furthermore the *r5.7* gene was detected by PCR in the non-virulent strains 7T7_10 and 8T7_10 that carry the pGV plasmid (Figure 1,

142 black squares). Together these results indicate a role for pGV in virulence but additional genomic
143 components appear to be necessary.
144
145 **Oysters act as reservoir of the *V. crassostreae* pathogen**
146 *V. crassostreae* infection has been recurrently associated with POMS events that affect juvenile
147 oysters at a temperature threshold of 16°C (Bruto et al., 2017, de Lorgeril et al., 2018, Lemire et
148 al., 2015). In oyster farming areas such as Brest, roughly 700 tons of farmed oysters are
149 introduced into a site where 10'000 tons of wild oysters reside (Pouvreau, personal
150 communication). We thus asked whether oysters may asymptomatically host *V. crassostreae* and
151 hence play a role as a reservoir of this pathogen. Wild adult animals were collected from Brest at
152 12°C and returned to the laboratory where they were transferred into a tank at 21°C, a procedure
153 previously shown to allow the development and transmission of oyster diseases (Petton et al.,
154 2015a, Petton et al., 2015b, Petton et al., 2013). Mortality started at day 8, reached 90% after day
155 14, and were accompanied by the presence of *V. crassostreae* in the water tank and in the
156 hemolymph of moribund animals (Figure S3). The pGV plasmid was detected in 39 of 41 (95%)
157 *V. crassostreae* strains isolated during this experiment. We noted that *V. aestuarianus* was not
158 isolated on *Vibrio* selective media (TCBS, see material and method), although it was detected by
159 PCR in animal tissues, co-occurring or not with *V. crassostreae*. On the other hand, OsHV-1 was
160 never detected in DNA extracted from the oysters. Contaminated seawater (CSW) was collected
161 at day 11 from the tank containing the moribund wild oysters and three-month-old specific
162 pathogen free oysters (SPF juveniles) were exposed to this CSW at 21°C (Petton et al., 2013).
163 Mortalities of the juveniles started at day 3 and reached 100% after 6 days. No mortality occurred
164 when SPF juveniles were kept in filtered seawater at the same temperature. *V. crassostreae* and
165 *V. aestuarianus,* but not OsHV-1, were detected in moribund animal tissues. These results

showed that wild adult oysters are reservoirs of virulent *V. crassostreae* and increasing the temperature can induce disease symptoms.

A transcriptional regulator is necessary for pGV-mediated virulence and cytotoxicity.

Having shown that oyster farming correlates with a high prevalence of the virulence plasmid, we next explored the virulence trait(s) encoded by pGV. A previous study identified a region within pGV (Px3, Figure 2A) that is necessary for virulence in *V. crassostreae* (Bruto et al., 2017). Manual annotation of the genes within this region did not reveal any known virulence determinants, but a putative transcriptional regulator (labelled VCR9J2v1_750086 in J2-9 and hereafter named TF for simplicity) was identified. We assessed the importance of TF for virulence using a genetic knockout approach. Deletion of this gene (Δtf) resulted in a significant decrease in mortality after oyster injection (Figure 2B). Constitutive expression of *tf* from a plasmid was sufficient to restore virulence both in the Δtf mutant and in a mutant lacking the complete Px3 region (ΔPx3). On the other hand, expression of *tf* in a pGV-cured strain did not result in increased mortality (Figure 2B). These results showed that the gene encoding the TF regulator is the only gene involved in Px3-mediated virulence but that additional determinant(s), carried by this plasmid, are involved in *V. crassostreae* virulence.

V. crassostreae virulence has been recently demonstrated to be intimately related with its cytotoxic effects on hemocytes (Rubio et al., in press). Here, using flow-cytometry, we observed that *V. crassostreae* effects on hemocyte viability require the presence of pGV. Deletion of the Px3 region or of the *tf* gene also led to an attenuation of cytotoxicity (Figure 2C). Expression of the *tf* gene *in trans* complemented the ΔPx3 deletion with respect to hemocyte toxicity, mirroring

the phenotype observed following oyster injection. This result was surprising as pGV was previously described as dispensable for *V. crassostreae* cytotoxicity (Rubio et al., in press). This discrepancy might be explained by the different methodological approaches used to assess cell viability. In the previous study, bacteria were added to hemocyte monolayers at a multiplicity of infection (MOI) of 50 and viability monitored for 15 hours by a Sytox green assay (Rubio et al., in press). Here, exposition of hemocytes to vibrios was performed in a cell suspension at a MOI of 10 for 6 hours before addition of SYBR Green-I and propidium iodide to determine cell viability by flow cytometry. To verify that the plasmid is essential for toxicity, we thus incubated the hemocytes with a wild type *V. crassostreae* strain (J2-9) or with a plasmid-cured strain (ΔpGV) at MOIs of 10 or 100 for 6 hours. These tests revealed a dose-dependent effect in which low levels of the plasmid-cured strain were less cytotoxic while high levels could overcome the plasmid deficiency (Figure S4). Altogether, our results showed that the TF regulator controls plasmid-carried genes involved in hemocyte cytotoxicity.

The TF transcriptional regulator activates a Type 6 Secretion System (T6SS).

The *tf* gene encodes a putative transcriptional regulator of the AraC family that contains two domains: a N-terminal domain with putative Class I glutamine amidotransferase function and a C-terminal helix-turn-helix DNA binding domain (Figure S5). To identify its target gene(s) we conducted a RNAseq analysis to compare the transcriptomes of a *V. crassostreae* derivative ΔPx3 constitutively expressing either the *tf* or the gene encoding the green fluorescent protein (*gfp*), as a control. Expression of *tf* resulted in significant changed mRNA levels for only 27 predicted protein-coding genes (Log2Fold change >2, Table S4) of which 6 and 21 genes were down- and up-regulated, respectively, in a TF-dependent manner. All 21 up-regulated genes were located on

the virulence plasmid and encode a putative T6SS (here after named $T6SS_{pGV}$) (Figure 3). The induction of two of the $T6SS_{pGV}$ genes (*vipA* and *vgrG*, the first gene of each operon) by TF was further validated by RT-PCR in two biologically independent experiments (Figure S6).

The $T6SS_{pGV}$ locus is organized into at least two operons with *vgrG*, a gene encoding unknown function and *paar* being expressed in the opposite direction compared to the rest of the $T6SS_{pGV}$ genes. Between these two operons, we predicted a bidirectional promoter (-10/-35 boxes on each operon site) as well as a putative TF target site that comprised a palindromic sequence of 6 nucleotides spaced by 5 nucleotides (Figure 4). This motif was not identified at other loci within the *V. crassostreae* genome. To test whether the transcription factor and this putative promoter region were sufficient to drive expression of adjacent genes in a heterologous host, we cloned the promoter between GFP- and DsRed-encoding genes in a replicative plasmid. Next, we transformed this reporter plasmid into an unrelated *Vibrio* species (in this case *V. cholerae*), which had been engineered to chromosomally encode *tf* under the control of an arabinose-inducible promoter (P_{BAD}) (see Materials and methods for details). Induction of *tf* expression by arabinose resulted in the production of both GFP and DsRed demonstrating that the promoter was indeed bidirectional and activated by TF (Figure 4). Deletion of the palindromic sequence altered the induction capacity of TF, while inversion or mutation of one of the 6 nucleotide sites did not abrogate gene activation (Figure 4). We therefore concluded that the TF transcription factor drives T6SS expression in *V. crassostreae.*

The $T6SS_{pGV}$ is involved in virulence and hemocyte cytotoxicity

T6SSs are contact-dependent contractile nanomachines used by many Gram-negative bacteria as weapons against a variety of prokaryotic and eukaryotic organisms (Cianfanelli et al., 2016).

Indeed, T6SSs allow bacteria to translocate a wide variety of toxic effectors into target cells. Formed by a minimum of 13 conserved 'core' components, T6SSs are made up of three large sub-structures: a trans-membrane complex, a baseplate and a tail composed of an inner tube formed by hexamers of hemolysin-coregulated protein (Hcp) encased within an outer VipA/VipB sheets complex and topped with a VgrG spike, which can be extended by a final tip formed by a PAAR-motif protein. T6SS effectors are frequently fused to C-termini of T6SS structural proteins, such as VgrG or PAAR (Shneider et al., 2013). However, *in silico* analysis did not predict any C-terminal extension of the VgrG or PAAR proteins of *V. crassostreae.* We also failed to identify any putative effector protein using a public database (http://db-mml.sjtu.edu.cn/SecReT6/).

A genetic approach was therefore used to test the importance of the $T6SS_{pGV}$ for *V. crassostreae* virulence. We had previously generated a knockout mutant that lacked this locus and observed no effect on virulence (Bruto et al., 2017). However, re-investigating this mutant we identified an unexpected duplication of this region resulting in one deleted and one whole T6SS cluster. Several attempts to delete the *vgrG* or *vipA* genes were unsuccessful, repeatedly resulting in complete loss of the plasmid, suggesting that these mutations come at a cost for the bacteria. However, deletion of the T6SS *paar* gene was successful (Δ*paar*) and led to decreased virulence (Figure 2A). Complementation by constitutively expressing *paar in trans* restored the virulence potential to similar levels as observed for the WT.

Having demonstrated a role for the T6SS in virulence, we next explored its cellular target. In many bacterial models, T6SSs are used to kill competing bacteria (Cianfanelli et al., 2016). We

thus asked whether *V. crassostreae* that constitutively expressed *tf* would be able to kill bacteria in an *in vitro* killing assay (Borgeaud et al., 2015). When the *tf*-expressing strain was used as a predator and *E. coli*, *V. cholerae*, or a collection of 40 diverse *Vibrio* strains isolated from oysters were used as prey, we did not observe any killing under the tested conditions. The T6SS has also been demonstrated to mediate toxicity for eukaryotic cells. For example, non-pandemic *V. cholerae* exhibits T6SS-mediated cytotoxicity towards macrophages and the soil amoeba *Dictyostelium discoideum* (Pukatzki et al., 2007), while the aquatic amoebae *Acanthamoeba castellanii* is not affected (Van der Henst et al., 2018). Here, we observed that the *V. crassostreae* Δ*paar* mutant has decreased cytotoxicity towards hemocytes compared to the WT and that expression of the *paar* gene *in trans* partially restored cytotoxicity (Figure 2C). Our results therefore suggest a critical role for the virulence plasmid, TF, and $T6SS_{pGV}$ in *V. crassostreae*-mediated killing of oyster immune cells and therefore pathogenicity towards this animal host.

Looking at the distribution of the $T6SS_{pGV}$ in publicly available *Vibrio* genomes, we found that closely related loci are present in *V. aestuarianus* (11/11 genomes) and *V. tapetis* (1/1 genome), which are pathogens of adult oysters and clams, respectively (Travers et al., 2015). Overall the synteny and amino acid identities between core components of the T6SSs were high with the exception of genes localized after the *vasK* gene that could be candidate effectors (Figure 5). In *V. aestuarianus*, a specific gene (VIBAEv3_A30819 in the strain 02-041) encodes a protein with weak sequence identity (25%) with a T3SS effector from *Bordetella bronchiseptica* named BteA. This secreted protein has been reported to inhibit phagocytosis by macrophage and induce necrosis through an actin cytoskeleton-signalling pathway (Kuwae et al., 2016). In the $T6SS_{pGV}$ a specific gene (VCRJ2v1_750073 in strain J2-9) encodes a protein with 38% similarity and 13% identity to the C-terminal and N-terminal domains of an insecticidal delta-endotoxin found in

Bacillus thuringiensis. Unfortunately, deletion of this gene in *V. crassostreae* also resulted in loss of pGV preventing further functional analysis. An ortholog of VCRJ2v1_750073 in *V. tapetis* has been pseudogenized, potentially leading to its functional inactivation. On the other hand, a second, species-specific gene in the *V. tapetis* T6SS encodes a protein with only 60% similarity and 29% identity within 45 amino acids of the central domain of nigritoxin, a toxin for crustaceans and insects (Labreuche et al., 2017). Hence while annotation and localization of these genes suggests a role as T6SS effectors for the three pathogens, the formal demonstration of their function remains to be done.

The T6SS$_{pGV}$ and R5.7 protein act independently to mediate *V. crassostreae* cytotoxicity

We showed in a previous study (Bruto et al., 2018) that *V. crassostreae* evolution as pathogen involved sequential acquisition of virulence genes, including i) acquisition of the *r5.7* gene, which encodes an exported protein that may be involved in the contact-dependant cytotoxicity (Rubio et al in press) and ii) more recent acquisition of T6SS$_{pGV}$ that, in our experimental design, appeared necessary for the killing of host immune cells. It is therefore tempting to hypothesize that these two virulence traits work in concert to mediate cytotoxicity, R5.7 potentially favouring attachment of the vibrio to the hemocyte and facilitating anchorage of the T6SS$_{pGV}$, which then injects a toxic effector into the cell. Under such an hypothesis, deletion of the *r5.7* gene (Δr5.7) or curing of the plasmid (ΔpGV) should decrease the cytotoxicity of *V. crassostreae* to a similar level to that observed with the double mutant ΔpGV1512Δr5.7. However, as we observed that the cytotoxicity of the double mutant was significantly more attenuated than that of the single mutants (Figure 6), we suggest that these virulence factors act additively rather than being functionally connected.

DISCUSSION

In recent years, a syndrome affecting juveniles of *Crassostrea gigas* (POMS) has become panzootic, being observed in all coastal regions of France and numerous other countries worldwide, threatening the long-term survival of commercial and natural stocks of oysters (Le Roux et al., 2015). A study recently demonstrated that this syndrome results from an intense replication of the oyster herpes virus OsHV-1 µVar, creating an immune-compromised state that permits secondary infections by opportunistic bacteria (de Lorgeril et al., 2018). An unresolved question, however, is whether diverse bacterial species can be considered to be opportunistic or whether specific bacterial species cooperate to induce this syndrome. Here, we provide evidence that *V. crassostreae* is a major player of this syndrome. First, we propose that the recurrent detection of *V. crassostreae* in an area affected by POMS might indicate that it originates from a reservoir in oysters. Second, a high prevalence of a virulence plasmid is observed in oysters affected by POMS, suggesting that strains carrying this plasmid have a selective advantage. Third, cellular characterization of virulence traits sequentially acquired by *V. crassostreae,* revealed a lethal activity on hemocytes by distinct pathways.

Oyster-associated vibrios have been previously analyzed in the context of a metapopulation framework, *i.e.*, by considering potential overlap or differences in populations collected from spatially and temporally distinct habitats, which are connected by dispersal (Bruto et al., 2017). This study showed that *V. crassostreae* was abundant in diseased animals while nearly absent in the surrounding seawater, suggesting that its primary habitat is not the water column. Potential alternative reservoirs for *V. crassostreae* at temperature <16°C were still undetermined. Here, we showed that oysters that reside in farming areas year-round asymptomatically host

328 *V. crassostreae* and hence potentially serve as a pathogen reservoir. An increase of temperature
329 triggered active multiplication of *V. crassostreae* leading to a sufficiently high bacterial load
330 and/or virulence state allowing the pathogen to colonize and infect juvenile oysters. As *V.*
331 *aestuarianus* was detected in both adult and the juvenile oysters, it is impossible to discriminate
332 the respective roles of *V. crassostreae* and *V. aestuarianus* in the induction of oyster mortality in
333 the present experiment. It should be notice, however, that *V. aestuarianus* virulence seems to be
334 restricted to the adult stage of oyster (Azema et al., 2017). Importantly, OsHV-1 µVar was never
335 detected in our experiments, confirming previous observations that infection of juveniles can
336 occur in the absence of OsHV-1µVar (Petton et al., 2015b). Hence our present results suggest that
337 oyster mortality syndrome might have different etiologies. It remains to be determined how
338 temperature acts on *V. crassostreae* infective status. In the context of global warming, how
339 temperature influences the virulence of these pathogens as well as oyster resistance or resilience
340 is a major concern to predict sustainability of commercial and natural stocks of this species.
341
342 Another argument strengthening a role for *V. crassostreae* in oyster juvenile mortality syndrome
343 is the high frequency of the pGV plasmid in farming areas that are affected by the syndrome.
344 Although we were able to isolate *V. crassostreae* from oysters in Sylt, none of these isolates were
345 virulent in an infection assay. This observation is consistent with the absence of the pGV plasmid
346 in these isolates and strengthens our hypothesis that the introgression of pGV into the *V.*
347 *crassostreae* population has played a major role in its emergence as a pathogen (Bruto et al.,
348 2017). By identifying virulence traits of *V. crassostreae* encoded by this plasmid, *i.e.* the
349 $T6SS_{pGV}$ and its transcriptional activator TF, we deciphered a mechanism that increases
350 hemocyte cytotoxicity of *V. crassostreae* worsens oyster disease. In the future, identification of
351 the effector protein(s) of the $T6SS_{pGV}$ should help decipher its effect on hemocytes. In addition,

exploring the role of the T6SSs and its effector(s) in the virulence of *V. aestuarianus* and *V. tapetis* may support a parallel evolution from harmless to pathogenic states of these mollusk pathogens.

We also demonstrated that the T6SS and R5.7 are not co-dependent for their function, ruling out the hypothesis that R5.7 acts as a facilitator of T6SS-mediated injection of a toxic effector into hemocytes. Within the Splendidus clade, a few populations have lost the *r5.7* gene and are not able to kill oysters (Bruto et al., 2018). When infecting the host, these non-virulent strains are highly controlled by cellular (phagocytosis) and humoral (antimicrobial peptides, reactive oxygen species, and heavy metals) immunity mediated by the hemocytes (Rubio et al., in press). However, several *V. tasmaniensis* strains isolated from diseased oysters (Le Roux et al., 2009, Lemire et al., 2015) that do not carry the *r5.7* gene, were able to induce mortalities when injected to oysters. Compared to *V. crassostreae*, the hemocyte cytotoxicity of these strains was demonstrated to be dependent on phagocytosis and required a distinct T6SS localised on the chromosome 1 of the strain LGP32 ($T6SS_{Chr1\text{-}LGP32}$, Rubio et al in press) (Figure 5C). Consideration of this data led to the hypothesis that R5.7 may act as an inhibitor of phagocytosis and *V. tasmaniensis* secondary evolved as pathogen by the acquisition of $T6SS_{Chr1\text{-}LGP32}$ that is active at the intracellular stage as described for the *V. cholerae* T6SS (Ma et al., 2009). Alternatively, the acquisition of a $T6SS_{Chr1\text{-}LGP32}$ that is functions exclusively during the intracellular stage may have further selected for *r5.7* loss. Hence in addition to Rubio et al. article, the present study suggests multiple evolutionary scenarios leading to the emergence of pathogenic populations with common and specific virulence traits converging on a common objective: killing of the major actors of the oyster immune response. Finally our results confirm the functional diversity of the T6SS nanomachine and its effectors, acting against bacterial

competitors (Unterweger et al., 2014) against amoeba or phagocytic cells at an intracellular stage (Ma et al., 2009) or directly by contact with the target eukaryotic cell.

MATERIAL AND METHODS

Isolation of bacteria and gene sequencing

In July 2015 and 2016, 24 live oysters, together with surrounding seawater (temperature 18°C), were collected in Sylt. To collect zooplankton, large phytoplankton and organic particles, a 50 L sample was filtered through a 60 µm plankton net and the collected material was subsequently washed with sterile seawater. Small organic particles and free-living bacterial cells were collected from 2L water samples pre-filtered through the 60 µm plankton net and sequentially filtered through 5 µm, 1 µm and 0.22 µm pore size filters. These filtrates were directly placed onto *Vibrio* selective media (Thiosulfate-citrate-bile salts-sucrose agar, TCBS). The zooplankton and oyster tissues were ground in sterile seawater (10 mL/g of wet tissue) and streaked onto TCBS. About 150 colonies per seawater fraction and 300 colonies per oyster tissue sample were randomly picked and re-streaked on TCBS first and subsequently on Zobell agar (15 g/l agar, 4 g/l bactopeptone and 1 g/l yeast extract in artificial sea water, pH 7.6). All isolates were genotyped by partial *hsp60* gene sequencing and stored in 10% DMSO at -80°C. A total of 910 *hsp60* sequences were obtained from the two samplings performed in Sylt. This set of data was complemented with 719 *hsp60* sequences obtained from previous samplings at Brest in 2014 (Bruto et al., 2017) and 2016 (seawater temperature above 18°C).

Strains, plasmids and culture conditions. The strains used in this study are described in Table S5. *Vibrio* isolates were grown at 20°C in Zobell broth or agar, Luria-Bertani (LB) or LB-agar (LBA) + 0.5M NaCl. *Vibrio cholerae*, strain A1552, was grown in LB at 30°C. *Escherichia coli* strains were grown at 37°C in LB or on LBA. Chloramphenicol (5 or 25μg/ml for *Vibrio* and *E. coli*, respectively), spectinomycin (100μg/ml), kanamycin (75ug/ml for *V. cholerae*), thymidine (0.3 mM) and diaminopimelate (0.3 mM) were added as supplements when necessary. Induction of the P_{BAD} promoter was achieved by the addition of 0.2% L-arabinose to the growth media, and conversely, was repressed by the addition of 1% D-glucose where indicated.

Vector construction and mutagenesis. All plasmids used or constructed in the present study are described in Table S6. Deletion of selected regions or genes was performed by allelic exchange using the pSW7848T suicide plasmid (Le Roux et al., 2007, Val et al., 2012). To this end, two 500 bp fragments flanking the target region or gene were amplified, (see primer details in Table S7), assembled by PCR and cloned into pSW7848T as previously described (Lemire et al., 2015). The suicide plasmid was then transferred by conjugation from *E. coli* as donor to *Vibrio* as recipient. Subsequently, the first and second recombinations leading to pSW7848T integration and elimination were selected on Cm/glucose and arabinose containing media, respectively. For the complementation experiments, genes were cloned into the Apa1/Xho1 (*paar*) or EcoR1/Xho1 (TF) sites of the pMRB plasmid, which is stable in *Vibrio spp.* (Le Roux et al., 2011), resulting in constitutive expression from a P_{lac} promoter. Conjugations between *E. coli* and *Vibrio* were performed at 30°C as described previously (Le Roux et al., 2007). The T6SS intergenic region (i.e. putative promoter region) was PCR amplified, digested, and cloned into *Sma*I and *Stu*I sites in pBR-GFP_dsRed (Lo Scrudato and Blokesch, 2012) before being transferred to the *V. cholerae* strain A1552 carrying the arabinose-inducible *tf* on a mTn7 transposon. Mutagenesis of

423 the palindromic region was performed by PCR assembly as described earlier (Matsumoto-
424 Mashimo et al., 2004).
425
426 **Fluorescence microscopy**
427 *V. cholerae* cells were back-diluted (1:100) from an overnight culture and grown for 2h at 30C in
428 LB medium containing kanamycin. At this point, 0.2% arabinose was added to the culture where
429 indicated and the growth was continued for 2h before the bacteria were mounted onto agarose
430 pads (in 1% PBS) and imaged with a Plan-Apochromat 100×/1.4 Ph3 oil objective using a Zeiss
431 Axio Imager M2 epifluorescence microscope. Image acquisition occurred with the Zeiss
432 AxioVision software. Depicted images are representative of three independent biological
433 replicates.
434
435 **SDS-PAGE and Western blotting**
436 *V. cholerae* cells were grown for 5h at 30C in LB medium with or without 0.2% arabinose
437 supplementation (after 3h of growth) to induce *tf* in the respective strains. Cells were lysed by
438 resuspension in 2x Laemmli buffer (100 µl of buffer per OD_{600} unit of 1) and boiling at 95˚C for
439 15 min. Proteins were separated by SDS-PAGE (10% resolving gels) and blotted onto PVDF
440 membranes. Detection of proteins was carried out as described (Lo Scrudato and Blokesch, 2012)
441 using primary antibodies against GFP (Roche, #11814460001; diluted 1:5'000) and mCherry
442 (BioVision, #5993-100; diluted 1:5’000). Anti-mouse-HRP (Sigma, #A5278; diluted 1:20'000)
443 and anti-rabbit-HRP (Sigma, #A9169; diluted 1:20'000) were used as secondary antibodies. An
444 anti-RNA Sigma70-HRP conjugate (BioLegend; # 663205; diluted 1:10’000) was used to
445 validate equal loading. Lumi-Light^{PLUS} (Roche) served as an HRP substrate and the signals were

detected using a ChemiDoc XRS+ station (BioRad). Western blots were performed three independent times with comparable results.

Experimental infections.

Animals.

Three-month-old Specific Pathogen Free (SPF) oysters were descendants of a pool of 100 genitors that were produced in a hatchery under highly controlled conditions to minimize the influence of genetic and environmental parameters that could affect host sensitivity to the disease (Petton et al., 2015a, Petton et al., 2015b, Petton et al., 2013). These animals were used for experimental infections by immersion (see below) or by intramuscular injections of bacteria into the adductor muscle. Triploid adult oysters (24 to 30-months-old) were provided by a local oyster farm (Coïc, Pointe du Château, Logonna-Daoulas, France) and were used to collect hemolymph for cytotoxicity assays. Wild adult *C. gigas* oysters (n=50) were collected from Bay of Brest (Pointe du Château, 48° 20′ 06.19″ N, 4° 19′ 06.37″ W) in April 2019 (seawater temperature 12°C).

Disease monitoring in wild adult oysters.

After sampling in the Bay of Brest, wild adult oysters were immediately returned to the laboratory (Station Biologique de Roscoff, Roscoff, France). Upon arrival, the animals were first cleaned using a bristle brush and briefly rinsed to remove sand, sediments and other shell debris before being placed in a 300-L tank under static conditions (no change of seawater) with aerated 5-µm-filtered seawater at 21°C. Mortality was recorded daily for 14 days. Vibrios were isolated daily from the tank seawater (100 µl) or from the hemolymph of moribund animals (10 µl) by plating onto selective media (thiosulfate-citrate-bile salts-sucrose agar (TCBS), Difco, BD,

France). Randomly selected colonies were mixed into 20 µl of molecular biology grade water and heated using a thermal cycler (2720 thermal cycler, Applied Biosystems) at 98°C for 10 min and stored at −20°C for PCR testing.

Infection by immersion in contaminated seawater.

Contaminated seawater (CSW) containing the oyster-shed bacteria was obtained by sampling the seawater from the 300-L tank in which wild adult oysters had been held for 14 days. SPF oysters were transferred to aerated aquaria (20 oysters per 2.5 L aquarium) filled with either 1L CSW or with fresh 5-µm-filtered seawater as a control. Mortality was recorded daily for 6 days and moribund animals were removed and analysed for the presence of *V. crassostreae*, *V. aestuarianus* and OsHV-1.

Nucleic acid extraction and PCR

Hemolymph of moribund wild adult oysters was withdrawn from the adductor muscle using a 1 mL plastic syringe fitted with a 25-gauge needle, centrifuged for 5 min at 5000 rpm and the cell pellet kept at -20°C until further use. In the case of 3-month-old juvenile oysters, the whole wet body of dead animals was crushed in marine broth (1 mg/ml) using a Tissue Lyser II (Qiagen). Genomic DNA was purified from homogenized oyster tissues or hemocyte cell pellets by resuspension in lysis buffer (NaCl 0.1M, pH8 EDTA 0.025M, SDS 1%, proteinase K 100 µg/ml) for 16 h (56°C) followed by Phenol:Chloroform:Isoamyl Alcohol (Sigma-Aldrich, #77617) extraction.

The primer pairs and PCR conditions used for the detection of *V. crassostreae* (de Lorgeril et al., 2018), *V. aestuarianus* (Saulnier et al., 2010) and the herpes virus OsHV-1 (Martenot et al., 2010) have been described elsewhere. PCRs were performed on 300 ng oyster DNA for oyster

pathogen detection or on 1 µl cell lysate obtained from *Vibrio* randomly picked on TCBS for *V. crassostreae* identification.

Bacterial virulence determination by intramuscular injection.

Several cohorts of SPF-oysters were used to perform experimental infections by intramuscular injections of bacteria into the adductor muscle. Because the susceptibility to bacterial infection of these cohorts may have varied over the course of this study depending on biotic (size) and abiotic (temperature) parameters, each cohort was systematically submitted to an experimental infection by injection with 3 different concentrations (1X, 0.1X and 0.01X) of the pathogenic *V. crassostreae* wt strain J2-9 used here as a reference. The bacterial concentration determined to induce between 50-90% mortality was subsequently used on the considered cohort to evaluate bacterial virulence. Bacteria were grown under constant agitation at 20°C for 24 h in Zobell media. One hundred microliters of the culture (10^6 or 10^7 colony forming unit, cfu, depending on the susceptibility of the considered cohort) were injected intramuscularly into oysters. The bacterial concentration was confirmed by conventional dilution plating on Zobell agar. After injection, the oysters were transferred to aquaria (20 oysters per 2.5 L aquarium) containing 1 L of aerated 5 µm-filtered seawater at 20°C, and kept under static conditions. Experiments were performed in duplicate and repeated at least once. Mortality was assessed after 24 hours.

***In vitro* cytotoxicity assays**

Hemolymph was withdrawn from the adductor muscle through a notch previously ground in the oyster shell using a 1 mL plastic syringe fitted with a 25-gauge needle. After bleeding, syringes were maintained on ice and individually controlled by microscope observation to retain only

hemolymph that was free of contaminating particles (sperm, ovocytes, small debris...). Selected samples were filtered through a 80 μm mesh to eliminate aggregates or large pieces of debris (to avoid clogging of the flow-cytometer flow-cell) and pooled.

In order to adjust the bacteria/ hemocyte ratio, hemocyte and bacterial cell concentrations were measured by incubating 300 μL of the considered suspension (diluted at 10-2 in filtered sterile seawater, FSSW, in the case of bacterial suspensions) with SYBR®Green I (DNA marker, Molecular Probes, 10,000 × in DMSO) at 1× final concentration, in the dark at room temperature for 10 minutes before flow-cytometric analysis (FACSVerseTM, Becton Dickinson, CA, USA). Hemocytes or bacterial cells were detected on the FITC detector (527/32 nm) of the flow cytometer and their concentration calculated using the flow rate value given by the Flow-SensorTM device integrated to the flow cytometer.

After hemocyte counting, the hemolymph pool was divided into 200 μL sub-samples maintained on ice. Each sub-sample received 200 μL of the different bacterial suspensions (wild-type or derivatives) at a multiplicity of infection (MOI) of 10:1 or 200 μL of FSSW as a control. Each condition was tested in 3 replicates and the experiment was performed twice. Tubes were maintained at 18°C for 5.5 h. Then SYBR®Green I and Propidium Iodide (PI, Sigma–Aldrich) were added to each tube at final concentrations of 1× and 10 μg mL−1, respectively and incubation was continued for another 30 min (6h total incubation time): PI only permeates hemocytes that lose membrane integrity and are considered to be dead cells, whereas SYBR®Green I permeates both dead and living cells. SYBR Green and PI fluorescence were measured on the FITC detector (527/32 nm) and on the PerCP-Cy5-5 detector (700/54 nm) respectively. Results are expressed as percent dead hemocytes.

Genome sequencing, assembly, and annotation. Strains were sequenced (Plateforme genomique, Institut Pasteur, Paris; JGI) using Illumina HiSeq2000 technology with ~50-fold coverage as described previously (Lemire et al., 2015). Contigs were assembled *de novo* using Spades (Bankevich et al., 2012). Computational prediction of coding sequences together with functional assignments was performed using the automated annotation pipeline implemented in the MicroScope platform (Vallenet et al., 2013). Some gene annotations were manually curated using InterPro, FigFam, PRIAM, COGs, PsortB, TMHMM and synteny group computation. General features of the genome sequenced in the present study are presented Table S2.

***In silico* analyses.**

Species trees were reconstructed based on a MLST (Multi Locus Sequence Typing) containing 3 markers for *V. crassostreae* isolates phylogeny (*gyrB, rctB* and *rpoD*). Nucleotide sequences were aligned with Muscle and concatenated using Seaview (Gouy et al., 2010). Phylogenetic reconstruction was done using RAxML (Stamatakis, 2006) on this concatemer with the GTR model. Tree visualization was performed with iTOL (Letunic and Bork, 2011).

RNA-seq experimentation

The *Vibrio* strains J2-9 ΔPx3 constitutively expressing *tf* or *gfp* from a plasmid (pMRB) were grown in LB-NaCl. Bacteria were sampled at OD 0.3, 0.6 and 1.0 and RNA extraction was performed using TRIzol reagent and following manufacturer's instructions (Invitrogen). Total nucleic acids were quantified based on absorption at 260 nm and RNA integrity was verified by gel electrophoresis. DNA was removed by DNase I digestion using the Turbo DNA-free kit (Ambion). RNAs from the 3 OD conditions were pooled. The experiment was performed three

times. Directional cDNA libraries were constructed with the ScriptSeq RNA-Seq Library Preparation Kit (Illumina). Sequencing was done with the NextSeq 500/550 Mid Output Kit v2 (Illumina) on a NextSeq 500Mid (Illumina) by the "Plateforme de Séquençage haut-débit" at I2BC-UMR9198. Data treatment and mapping onto *V. crassostreae* J2-9 reference genome was performed with the TAMARA pipeline hosted by the MAGE platform (http://www.genoscope.cns.fr/agc/microscope/transcriptomic/NGSProjectRNAseq.php?projType=RNAseq).

Statistical analyses.

Survival of oysters after injection with the different genetic construct was analyzed by binomial generalized linear mixed models (GLMM) with logit link function taking the number of survivors vs. the number of dead oysters as response variable and strain identity as predictor. Due to the high number of cells analyzed in flow cytometry assays of hemocyte mortality, we used linear mixed models (LMM) with the proportions of alive and dead cells as response variable. Experimental trial was added as a random to account for differences between independent experiments when repeated trials were performed. To identify pairwise difference between strains we used simultaneous tests for general linear hypotheses implemented in the *multcomp* package (Hothorn et al., 2008) applying Tukey contrasts.

ACKNOWLEDGMENTS

We are grateful to Mark Cock (Marine station of Roscoff) for his thoughtful comments and english editing, which improved the manuscript. We thank the staff of the station Ifremer

Argenton and Bouin, the ABIMS and CRBM (Roscoff) and LABGeM (Evry) plateforms for technical assistance. This work was supported by grants from the Agence Nationale de la Recherche (ANR-16-CE32-0008-01 « REVENGE ») to FLR, Ifremer and the Region Bretagne to DP and AJ. MBl. is a Howard Hughes Medical Institute (HHMI) International Research Scholar (grant #55008726) and work in her group was supported by a Swiss National Science Foundation scientific exchange grant (IZSEZ0_181044) and an ERC Consolidator Grant from the European Research Council (724630-CholeraIndex).

REFERENCES

Azema, P., Lamy, J.B., Boudry, P., Renault, T., Travers, M.A., and Degremont, L. (2017) Genetic parameters of resistance to Vibrio aestuarianus, and OsHV-1 infections in the Pacific oyster, Crassostrea gigas, at three different life stages. Genet Sel Evol 49, 23.

Bankevich, A., Nurk, S., Antipov, D., Gurevich, A.A., Dvorkin, M., Kulikov, A.S., . . . Pevzner, P.A. (2012) SPAdes: a new genome assembly algorithm and its applications to single-cell sequencing. J Comput Biol 19, 455-477.

Borgeaud, S., Metzger, L.C., Scrignari, T., and Blokesch, M. (2015) The type VI secretion system of Vibrio cholerae fosters horizontal gene transfer. Science 347, 63-67.

Bruto, M., James, A., Petton, B., Labreuche, Y., Chenivesse, S., Alunno-Bruscia, M., . . . Le Roux, F. (2017) Vibrio crassostreae, a benign oyster colonizer turned into a pathogen after plasmid acquisition. ISME J 11, 1043-1052.

Bruto, M., Labreuche, Y., James, A., Piel, D., Chenivesse, S., Petton, B., . . . Le Roux, F. (2018) Ancestral gene acquisition as the key to virulence potential in environmental Vibrio populations. ISME J.

Cianfanelli, F.R., Monlezun, L., and Coulthurst, S.J. (2016) Aim, Load, Fire: The Type VI Secretion System, a Bacterial Nanoweapon. Trends Microbiol 24, 51-62.

de Lorgeril, J., Lucasson, A., Petton, B., Toulza, E., Montagnani, C., Clerissi, C., . . . Mitta, G. (2018) Immune-suppression by OsHV-1 viral infection causes fatal bacteraemia in Pacific oysters. Nat Commun 9, 4215.

Goudenege, D., Travers, M.A., Lemire, A., Petton, B., Haffner, P., Labreuche, Y., . . . Le Roux, F. (2015) A single regulatory gene is sufficient to alter Vibrio aestuarianus pathogenicity in oysters. Environ Microbiol 17, 4189-4199.

Gouy, M., Guindon, S., and Gascuel, O. (2010) SeaView version 4: A multiplatform graphical user interface for sequence alignment and phylogenetic tree building. Mol Biol Evol 27, 221-224.

Hothorn, T., Bretz, F., and Westfall, P. (2008) Simultaneous inference in general parametric models. Biom J 50, 346-363.

Kuwae, A., Momose, F., Nagamatsu, K., Suyama, Y., and Abe, A. (2016) BteA Secreted from the Bordetella bronchiseptica Type III Secetion System Induces Necrosis through an Actin Cytoskeleton Signaling Pathway and Inhibits Phagocytosis by Macrophages. PLoS One 11, e0148387.

Labreuche, Y., Chenivesse, S., Jeudy, A., Le Panse, S., Boulo, V., Ansquer, D., . . . Le Roux, F. (2017) Nigritoxin is a bacterial toxin for crustaceans and insects. Nat Commun 8, 1248.

631 Le Roux, F., Binesse, J., Saulnier, D., and Mazel, D. (2007) Construction of a Vibrio splendidus
632 mutant lacking the metalloprotease gene vsm by use of a novel counterselectable suicide
633 vector. Appl Environ Microbiol 73, 777-784.
634 Le Roux, F. and Blokesch, M. (2018) Eco-evolutionary Dynamics Linked to Horizontal Gene
635 Transfer in Vibrios. Annu Rev Microbiol 72, 89-110.
636 Le Roux, F., Davis, B.M., and Waldor, M.K. (2011) Conserved small RNAs govern replication
637 and incompatibility of a diverse new plasmid family from marine bacteria. Nucleic Acids Res
638 39, 1004-1013.
639 Le Roux, F., Wegner, K.M., Baker-Austin, C., Vezzulli, L., Osorio, C.R., Amaro, C., . . . Huehn,
640 S. (2015) The emergence of Vibrio pathogens in Europe: ecology, evolution, and pathogenesis
641 (Paris, 11-12th March 2015). Front Microbiol 6, 830.
642 Le Roux, F., Zouine, M., Chakroun, N., Binesse, J., Saulnier, D., Bouchier, C., . . . Mazel, D.
643 (2009) Genome sequence of Vibrio splendidus: an abundant planctonic marine species with a
644 large genotypic diversity. Environ Microbiol 11, 1959-1970.
645 Lemire, A., Goudenege, D., Versigny, T., Petton, B., Calteau, A., Labreuche, Y., and Le Roux, F.
646 (2015) Populations, not clones, are the unit of vibrio pathogenesis in naturally infected oysters.
647 ISME J 9, 1523-1531.
648 Letunic, I. and Bork, P. (2011) Interactive Tree Of Life v2: online annotation and display of
649 phylogenetic trees made easy. Nucleic Acids Res 39, W475-478.
650 Lo Scrudato, M. and Blokesch, M. (2012) The regulatory network of natural competence and
651 transformation of Vibrio cholerae. PLoS Genet 8, e1002778.
652 Ma, A.T., McAuley, S., Pukatzki, S., and Mekalanos, J.J. (2009) Translocation of a Vibrio
653 cholerae type VI secretion effector requires bacterial endocytosis by host cells. Cell Host
654 Microbe 5, 234-243.

655 Martenot, C., Oden, E., Travaille, E., Malas, J.P., and Houssin, M. (2010) Comparison of two
656 real-time PCR methods for detection of ostreid herpesvirus 1 in the Pacific oyster Crassostrea
657 gigas. J Virol Methods 170, 86-89.
658 Matsumoto-Mashimo, C., Guerout, A.M., and Mazel, D. (2004) A new family of conditional
659 replicating plasmids and their cognate Escherichia coli host strains. Res Microbiol 155, 455-
660 461.
661 Parizadeh, L., Tourbiez, D., Garcia, C., Haffner, P., Degremont, L., Le Roux, F., and Travers,
662 M.A. (2018) Ecologically realistic model of infection for exploring the host damage caused by
663 Vibrio aestuarianus. Environ Microbiol 20, 4343-4355.
664 Petton, B., Boudry, P., Alunno-Bruscia, M., and Pernet, F. (2015a) Factors influencing disease-
665 induced mortality of Pacific oysters Crassostreae gigas. Aquaculture Environ interact 6, 205-
666 222.
667 Petton, B., Bruto, M., James, A., Labreuche, Y., Alunno-Bruscia, M., and Le Roux, F. (2015b)
668 Crassostrea gigas mortality in France: the usual suspect, a herpes virus, may not be the killer
669 in this polymicrobial opportunistic disease. Front Microbiol 6, 686.
670 Petton, B., Pernet, F., Robert, R., and Boudry, P. (2013) Temperature influence on pathogen
671 transmission and subsequent mortalities in juvenile Pacific oysters Crassostrea gigas. Aquacult
672 Environ Interact 3, 257-273.
673 Pukatzki, S., Ma, A.T., Revel, A.T., Sturtevant, D., and Mekalanos, J.J. (2007) Type VI secretion
674 system translocates a phage tail spike-like protein into target cells where it cross-links actin.
675 Proc Natl Acad Sci U S A 104, 15508-15513.
676 Reise, K., Buschbaum, C., Buttger, H., Rick, J., and Wegner, K.M. (2017) Invasion trajectory of
677 Pacific oysters in the northern Wadden Sea. Mar Biol 164, 68.

678 Rubio, T. Oyanedel-Trigo, D., Labreuche, Y., Toulza, E. Luo, X., Bruto, M., Chaparro, C.,
679 Torres, M., de Lorgeril, J., Haffner, P., Vidal-Dupiol, J., Lagorce, A., Petton, B., Mitta, G.,
680 Jacq, A., Le Roux, F., Charrière, G., and Destoumieux-Garzón, D. Species-specific
681 mechanisms of cytotoxicity toward immune cells determine the successful outcome
682 of *Vibrio* infections. PNAS, In press
683 Saulnier, D., De Decker, S., Haffner, P., Cobret, L., Robert, M., and Garcia, C. (2010) A large-
684 scale epidemiological study to identify bacteria pathogenic to Pacific oyster Crassostrea gigas
685 and correlation between virulence and metalloprotease-like activity. Microb Ecol 59, 787-798.
686 Shapiro, B.J., Levade, I., Kovacikova, G., Taylor, R.K., and Almagro-Moreno, S. (2016) Origins
687 of pandemic Vibrio cholerae from environmental gene pools. Nat Microbiol 2, 16240.
688 Shneider, M.M., Buth, S.A., Ho, B.T., Basler, M., Mekalanos, J.J., and Leiman, P.G. (2013)
689 PAAR-repeat proteins sharpen and diversify the type VI secretion system spike. Nature 500,
690 350-353.
691 Stamatakis, A. (2006) RAxML-VI-HPC: maximum likelihood-based phylogenetic analyses with
692 thousands of taxa and mixed models. Bioinformatics 22, 2688-2690.
693 Travers, M.A., Boettcher Miller, K., Roque, A., and Friedman, C.S. (2015) Bacterial diseases in
694 marine bivalves. J Invertebr Pathol 131, 11-31.
695 Unterweger, D., Miyata, S.T., Bachmann, V., Brooks, T.M., Mullins, T., Kostiuk, B., . . .
696 Pukatzki, S. (2014) The Vibrio cholerae type VI secretion system employs diverse effector
697 modules for intraspecific competition. Nat Commun 5, 3549.
698 Val, M.E., Skovgaard, O., Ducos-Galand, M., Bland, M.J., and Mazel, D. (2012) Genome
699 engineering in Vibrio cholerae: a feasible approach to address biological issues. PLoS genetics
700 8, e1002472.

Vallenet, D., Belda, E., Calteau, A., Cruveiller, S., Engelen, S., Lajus, A., . . . Medigue, C. (2013) MicroScope--an integrated microbial resource for the curation and comparative analysis of genomic and metabolic data. Nucleic Acids Res 41, D636-647.

Van der Henst, C., Vanhove, A.S., Drebes Dorr, N.C., Stutzmann, S., Stoudmann, C., Clerc, S., . . . Blokesch, M. (2018) Molecular insights into Vibrio cholerae's intra-amoebal host-pathogen interactions. Nat Commun 9, 3460.

TITLES AND LEGENDS TO FIGURES

Figure 1. The presence of the pGV plasmid is correlated with the geographic origin and virulence of *V. crassostreae* strains. Phylogenetic tree of 89 *V. crassostreae* isolates based on the *gyrB*/*rctB*/*rpoD* gene fragments. Dark/light shades of gray indicate the two clades within the species. Rings, from inside to outside, indicate i) the geographic origin of the isolates (Brest, brown square; Sylt, beige square); ii) the presence (blue circles) or absence (white circles) of pGV-like plasmids; iii) the presence (black squares) or absence (white squares) of the *r5-7* gene and iv) the mortality rate (colour gradient from green to red corresponding to 0 to 100%) induced by individual strains 24h after injection in oysters (n=20). Experiments were performed in duplicate with two distinct oyster batches. The arrows highlight the virulent strains previously sequenced (Lemire et al., 2015) the non-virulent strain from clade 1(8T5_11) and the two plasmid-carrying but non-virulent strains from clade 2 (7T7_10 and 8T7_10).

Figure 2. Experimental assessment of pGV loci as virulence determinants. A-The indicated region or genes were deleted by allelic exchange and the virulence of *V. crassostreae* J2-9 wild-type (wt), mutants of specific loci (Δ) and complemented strains (+Plac_tf or paar) was compared by **B-** injection of strains (10^6 or 10^7 cfu depending on the cohort susceptibility, see Material and Methods) in 20 oysters and counting the percentage of mortalities after 24 hours; **C-** hemocyte cell viability evaluated by flow cytometry using a double staining procedure (SYBR® Green and propidium iodide, PI, Sigma). Injection and cell viability assays were performed in duplicate and triplicate, respectively, and reproduced at least twice. A single experiment is represented here for each method. Letters indicate significant differences of mortality assessed by simultaneous tests

731 for general linear hypotheses with Tukey contrasts ($P < 0.05$).

732

733 **Figure 3. The identified transcription factor activates both T6SS$_{pGV}$ operons.** RNAseq
734 analyses revealed that the expression of *tf* resulted in changed mRNA levels (Log2Fold change
735 on the y-axis) of 21 genes belonging to the T6SS$_{pGV}$ cluster (x-axis). The T6SS$_{pGV}$ locus is
736 organized into two putative operons expressed in opposite directions.

737

738 **Figure 4. The identified transcription factor activates a bidirectional promoter.** The putative
739 bidirectional promoter containing a palindromic sequence (shown in the middle in A) was cloned
740 between *gfp* and *dsRed* in a replicative plasmid, which was used to transform *V. cholerae* strain
741 A1552-TnTF1512. This strain carries *tf* behind an arabinose inducible promoter within a miniTn7
742 transposon. Induction of the transcription factor by arabinose resulted in the production of both
743 GFP and DsRed as observed by epifluorescence microscopy (B) or western blotting (C).

744

745 **Figure 5 Comparative genomic of *V. crassostreae V. aestuarianus* and *V. tapetis* T6SS and**
746 **putative effectors.** A. Synteny of the T6SS in the three strains compared. Genes with the same
747 colour code are homologous (>40% amino acid identity). Specific genes in each T6SS are shaded
748 in yellow and described in B. Schematic representation of the sequence identity or structural
749 similarity of the putative effector of *V. crassostreae* T6SS$_{pGV}$ in strain J2-9, *V. aestuarianus* 02-
750 041 and *V. tapetis* CECT4600. Structural similarities were identified with Phyre2. C. Phylogeny
751 based on a concatemer of T6SS homologs found in *V. crassostreae* (J5-4; LGP7; J2-9; J5-20), *V.*
752 *tapetis* (CECT4600), *V. aestuarianus* (07-115; 02-041; 12-128a; 01-032) and *V. tasmaniensis*

(LGP32; J0-13). The matrix shows the conservation of the different T6SS homologs with $T6SS_{pGV}$ as a reference. A scale bar indicating amino acid sequence identity is located to the right of the matrix.

Figure 6. Cytotoxic activities of T6SS and R5.7. The cytotoxicity of *V. crassostreae* wt or mutant strains (Δ) was assessed by flow cytometry using a double staining procedure. Control hemocytes were either incubated in the absence of any bacteria or with a non-virulent strain (J2-8). The experiment was performed in triplicate and reproduced twice. A single experiment is represented here. Letters indicate significant differences of mortality assessed by simultaneous tests for general linear hypotheses with Tukey contrasts ($P < 0.05$).

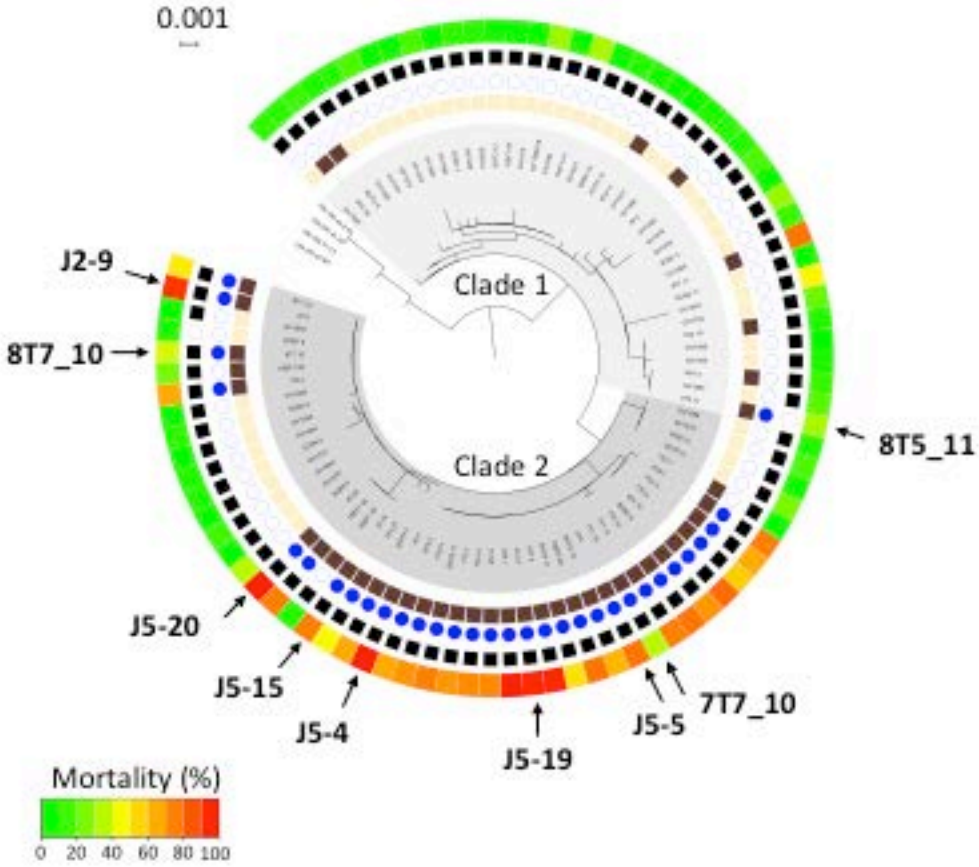
0.001
J2-9
8T7_10
Clade 1
Clade 2
8T5_11
J5-20
J5-15
J5-4
J5-19
J5-5
7T7_10
Mortality (%)
0 20 40 60 80 100

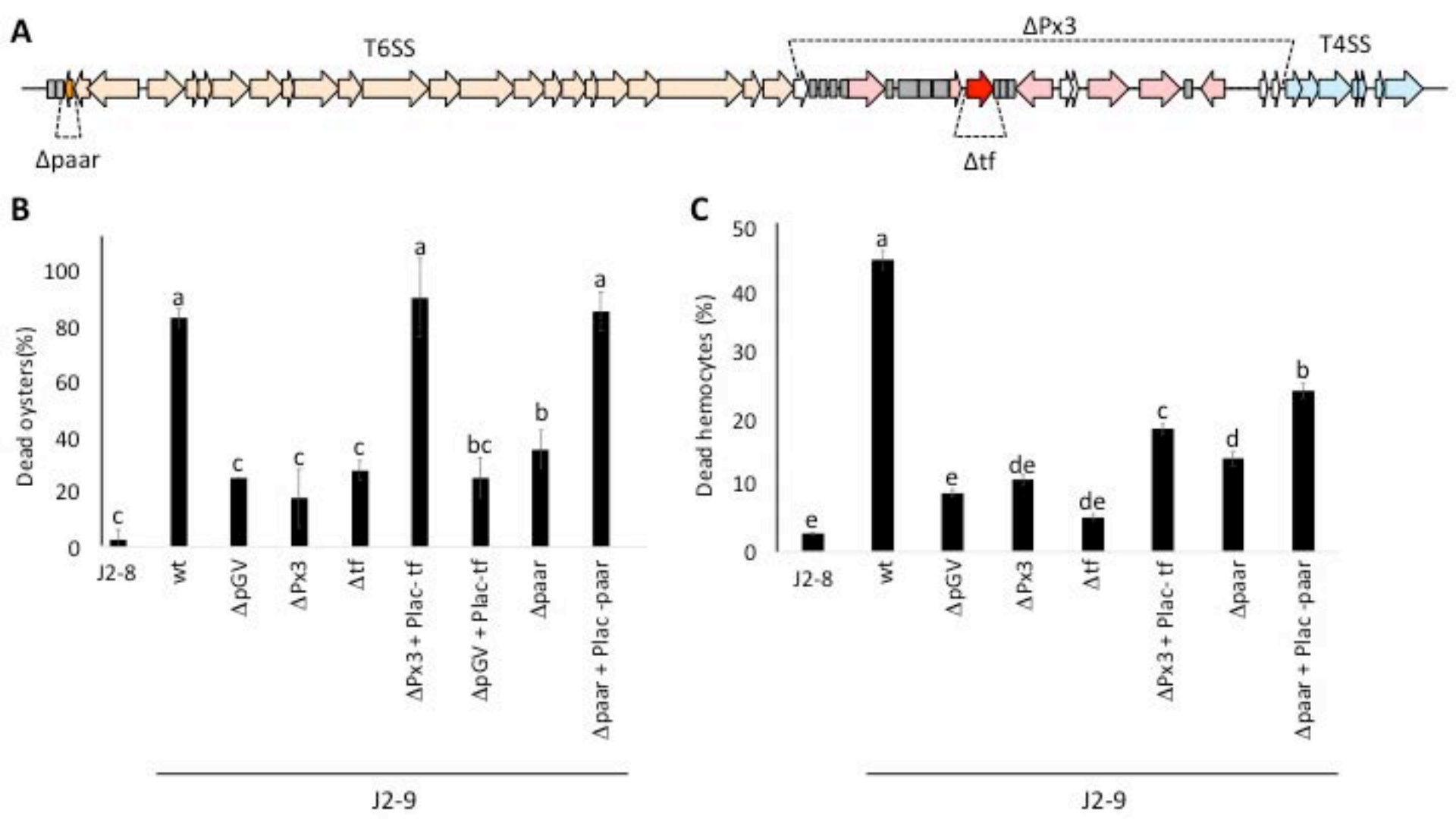
A
T6SS
ΔPx3
T4SS
Δpaar
Δtf
B
Dead oysters(%)
100
80
60
40
20
0
a
a
c
c
c
a
bc
b
a
c
J2-8
wt
ΔpGV
ΔPx3
Δtf
ΔPx3 + Plac-tf
ΔpGV + Plac-tf
Δpaar
Δpaar + Plac -paar
J2-9
C
Dead hemocytes (%)
50
40
30
20
10
0
a
e
e
de
de
c
d
b
J2-8
wt
ΔpGV
ΔPx3
Δtf
ΔPx3 + Plac-tf
Δpaar
Δpaar + Plac -paar
J2-9

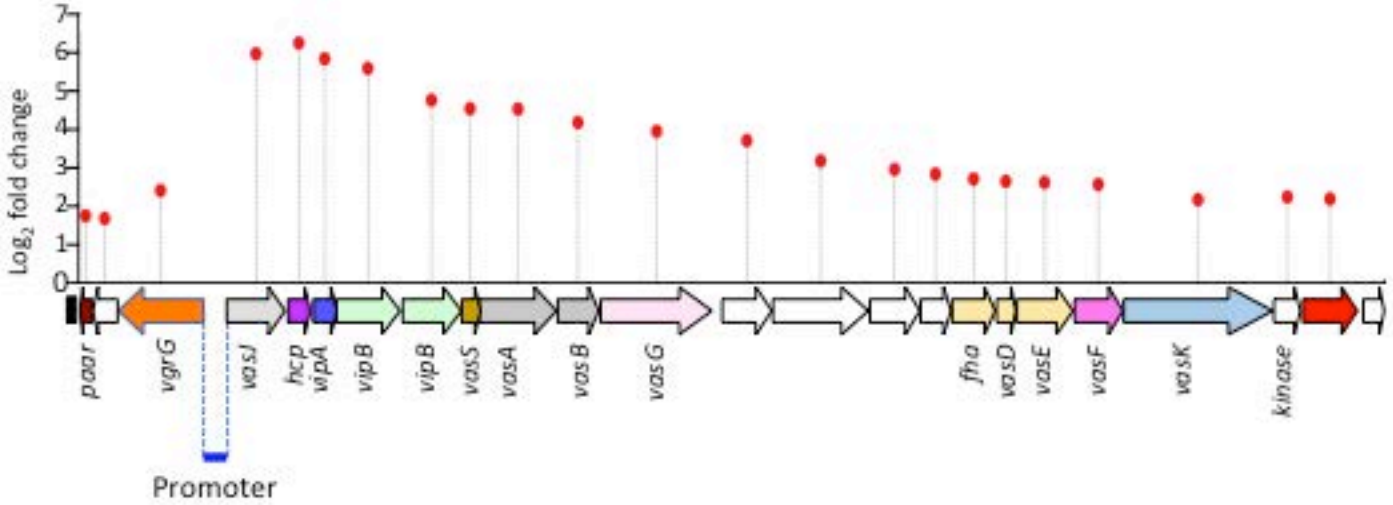
Log2 fold change
0
1
2
3
4
5
6
7
paar
vgrG
vasJ
hcp
vipA
vipB
vipB
vasS
vasA
vasB
vasG
fha
vasD
vasE
vasF
vasK
kinase
Promoter

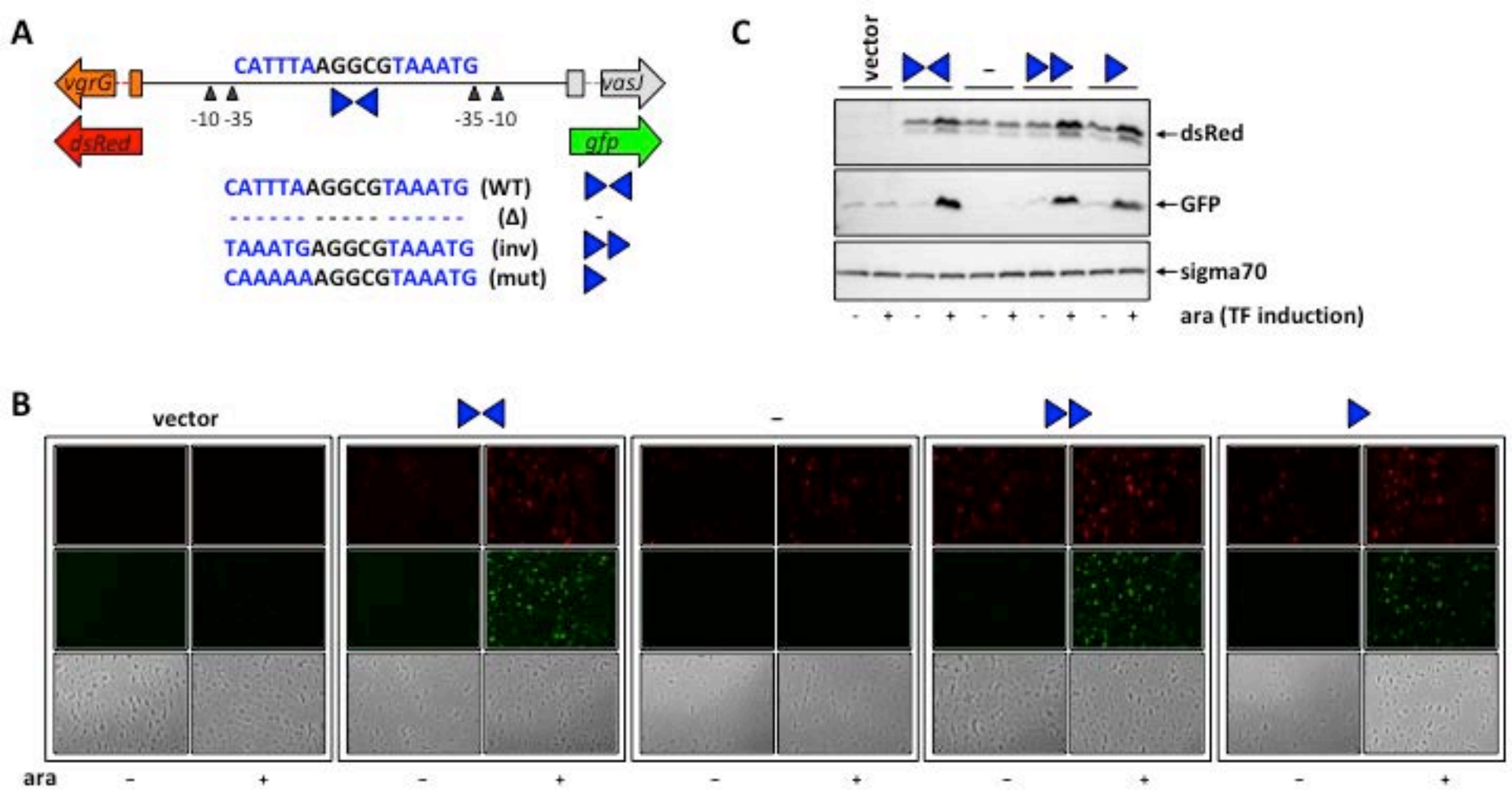
A
vgrG
CATTTAAGGCGTAAATG
vasJ
-10 -35
-35 -10
dsRed
gfp
CATTTAAGGCGTAAATG (WT)
(Δ)
TAAATGAGGCGTAAATG (inv)
CAAAAAAGGCGTAAATG (mut)
C
vector
dsRed
GFP
sigma70
ara (TF induction)
B
vector
ara

A

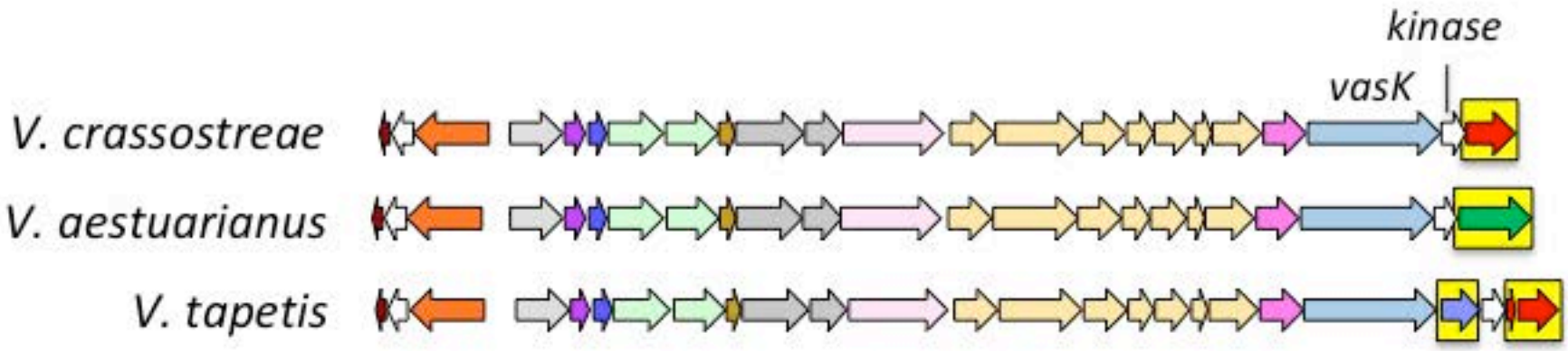
kinase
vasK
V. crassostreae
V. aestuarianus
V. tapetis

B

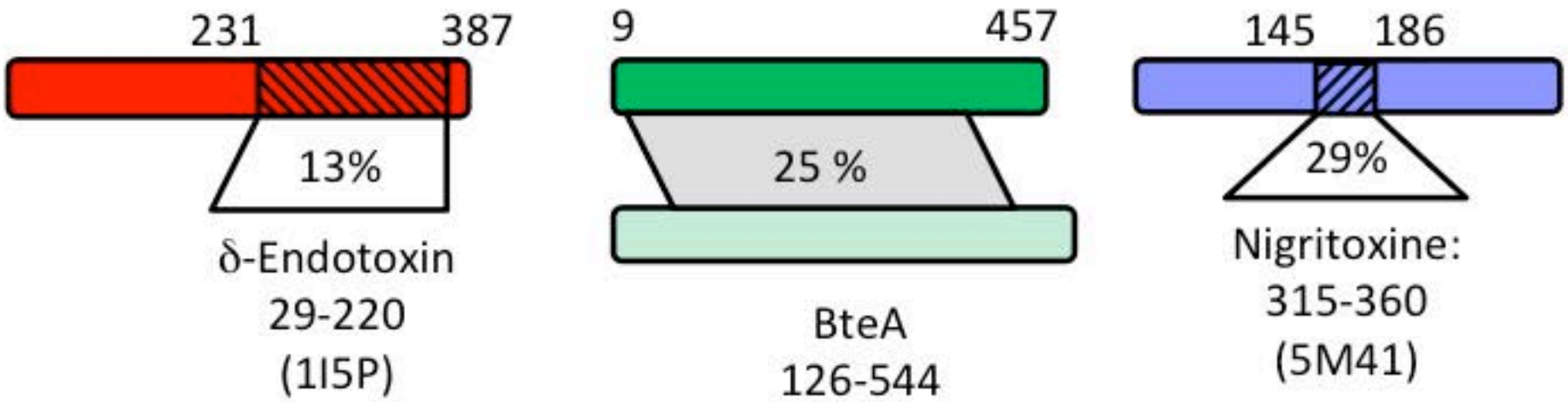
V. crassostreae
VCR9J2v1_750073
231
387
13%
δ-Endotoxin
29-220
(1I5P)
V. aestuarianus
VIBAEv3_A30819
9
457
25 %
BteA
126-544
V. tapetis
VIBTAv3_B0550
145
186
29%
Nigritoxine:
315-360
(5M41)

C

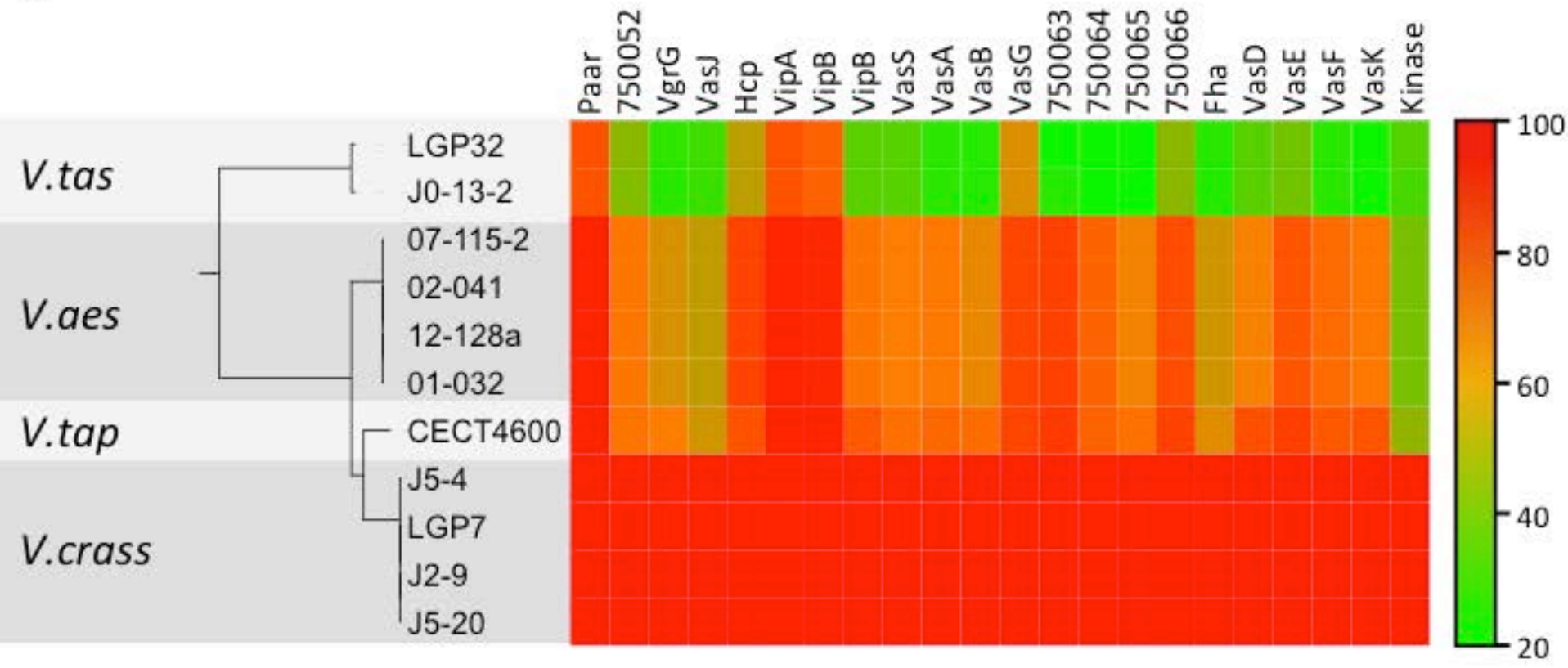
Paar
750052
VgrG
VasJ
Hcp
VipA
VipB
VipB
VasS
VasA
VasB
VasG
750063
750064
750065
750066
Fha
VasD
VasE
VasF
VasK
Kinase
V.tas
LGP32
J0-13-2
V.aes
07-115-2
02-041
12-128a
01-032
V.tap
CECT4600
V.crass
J5-4
LGP7
J2-9
J5-20
100
80
60
40
20

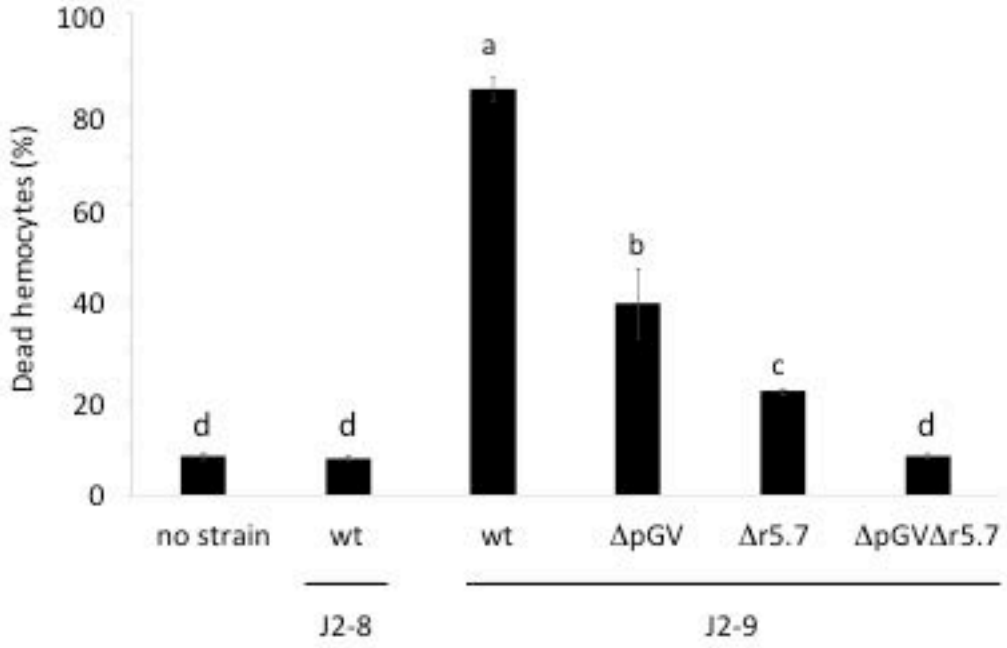
Dead hemocytes (%)
100
80
60
40
20
0
a
b
c
d
d
d
no strain
wt
wt
ΔpGV
Δr5.7
ΔpGVΔr5.7
J2-8
J2-9

Strains	Isolation site	Isolation date	Fraction	Plasmid	Oyster batch 1	
					Mortality (%)	Deviation
16BF1_28	Brest	2016	1-5 µM	0	20.0	14.1
16BF1_56	Brest	2016	1-5 µM	1	70.0	14.1
16BF1_95	Brest	2016	1-5 µM	0	5.0	0.0
16BF5_48	Brest	2016	5-1 µM	1	72.5	17.7
7F5_27	Brest	2014	5-1 µM	1	40.0	21.2
7G1_1	Brest	2014	Oyster	0	0.0	0.0
7P_6	Brest	2014	1-0.2 µM	0	7.5	0.0
7T1_10	Brest	2014	Oyster	1	30.0	0.0
7T1_12	Brest	2014	Oyster	1	70.0	7.1
7T3_1	Brest	2014	Oyster	1	65.0	7.1
7T4_11	Brest	2014	Oyster	1	60.0	14.1
7T4_12	Brest	2014	Oyster	1	72.5	3.5
7T5_9	Brest	2014	Oyster	1	52.5	3.5
7T6_10	Brest	2014	Oyster	1	67.5	3.5
7T8_1	Brest	2014	Oyster	1	60.0	7.1
7T8_11	Brest	2014	Oyster	1	65.0	7.1
8F5_39	Brest	2014	5-1 µM	0	7.5	10.6
8H1_4	Brest	2014	Oyster	0	10.0	7.1
8T1_12	Brest	2014	Oyster	1	45.0	7.1
8T2_1	Brest	2014	Oyster	1	92.5	3.5
8T2_10	Brest	2014	Oyster	0	5.0	7.1
8T2_4	Brest	2014	Oyster	1	67.5	3.5
8T5_10	Brest	2014	Oyster	1	75.0	14.1
8T5_11	Brest	2014	Oyster	1	27.5	10.6
8T7_10	Brest	2014	Oyster	1	35.0	7.1
8T7_11	Brest	2014	Oyster	0	22.5	3.5
8T7_4	Brest	2014	Oyster	1	90.0	7.1
8T8_11	Brest	2014	Oyster	0	2.5	3.5
8T8_2	Brest	2014	Oyster	1	60.0	0.0
8T8_7	Brest	2014	Oyster	1	70.0	0.0
BOB3_6	Brest	2016	Oyster	1	65.0	7.1
BOT2_10	Brest	2016	Oyster	1	57.5	3.5
BOT3_9	Brest	2016	Oyster	0	10.0	7.1
BOT4_11	Brest	2016	Oyster	1	47.5	10.6
BOT4_5	Brest	2016	Oyster	1	60.0	14.1
BOT5_11	Brest	2016	Oyster	1	70.0	0.0
J2-9	Brest	2011	Oyster	1	87.1	9.1
J5-15	Brest	2011	Oyster	1	70.0	14.1
J5-19	Brest	2011	Oyster	1	90.0	0.0
J5-20	Brest	2011	Oyster	1	92.5	3.5
J5-4	Brest	2011	Oyster	1	92.5	3.5

J5-5	Brest	2011	Oyster	1	72.5	24.7
16SF1_51	Sylt	2016	1-5 µM	0	27.5	24.7
16SF1_87	Sylt	2016	1-5 µM	0	0.0	0.0
S16	Sylt	2016	Oyster	0	25.0	14.1
GV1664	Sylt	2016	1-0.2 µM	0	0.0	0.0
GV1666	Sylt	2016	1-0.2 µM	0	0.0	0.0
GV1667	Sylt	2016	1-0.2 µM	0	0.0	0.0
GV1671	Sylt	2016	1-0.2 µM	0	2.5	3.5
GV1672	Sylt	2016	1-0.2 µM	0	2.5	3.5
GV1674	Sylt	2016	1-0.2 µM	0	12.5	3.5
GV1675	Sylt	2016	1-0.2 µM	0	12.5	3.5
GV1676	Sylt	2016	1-0.2 µM	0	0.0	0.0
GV1677	Sylt	2016	1-0.2 µM	0	0.0	0.0
GV1678	Sylt	2016	1-0.2 µM	0	12.5	3.5
GV1679	Sylt	2016	1-0.2 µM	0	0.0	0.0
GV1680	Sylt	2016	1-0.2 µM	0	7.5	3.5
GV1681	Sylt	2016	1-0.2 µM	0	0.0	0.0
GV1682	Sylt	2016	1-0.2 µM	0	7.5	3.5
GV1683	Sylt	2016	1-0.2 µM	0	0.0	0.0
GV1684	Sylt	2016	1-0.2 µM	0	5.0	0.0
GV1685	Sylt	2016	1-0.2 µM	0	7.5	3.5
GV1687	Sylt	2016	1-0.2 µM	0	15.0	7.1
GV1688	Sylt	2016	1-0.2 µM	0	0.0	0.0
GV1689	Sylt	2016	1-0.2 µM	0	12.5	3.5
GV1690	Sylt	2016	1-0.2 µM	0	10.0	0.0
GV1691	Sylt	2016	1-0.2 µM	0	0.0	0.0
GV1692	Sylt	2016	1-0.2 µM	0	5.0	0.0
GV1693	Sylt	2016	1-0.2 µM	0	42.5	3.5
GV1694	Sylt	2016	1-0.2 µM	0	2.5	3.5
GV1695	Sylt	2016	1-0.2 µM	0	5.0	0.0
GV1696	Sylt	2016	1-0.2 µM	0	5.0	7.1
GV1698	Sylt	2016	1-0.2 µM	0	0.0	0.0
GV1699	Sylt	2016	1-0.2 µM	0	10.0	7.1
GV1700	Sylt	2016	1-0.2 µM	0	17.5	10.6
GV1701	Sylt	2016	1-0.2 µM	0	7.5	10.6
SOB1_2	Sylt	2016	Oyster	0	25.0	14.1
SOB1_3	Sylt	2016	Oyster	0	0.0	0.0
SOB1_6	Sylt	2016	Oyster	0	2.5	3.5
SOB1_8	Sylt	2016	Oyster	0	5.0	7.1
SOB4_6	Sylt	2016	Oyster	0	30.0	7.1
SOB6_12	Sylt	2016	Oyster	0	7.5	3.5
SOB7_9	Sylt	2016	Oyster	0	7.5	10.6
SOS2_11	Sylt	2016	Oyster	0	0.0	0.0
SOS2_6	Sylt	2016	Oyster	0	7.5	3.5

SOS4_4	Sylt	2016	Oyster	0	5.0	0.0
SOT2_12	Sylt	2016	Oyster	0	0.0	0.0
SOT3_10	Sylt	2016	Oyster	0	0.0	0.0
SOT8_11	Sylt	2016	Oyster	0	20.0	7.1

Oyster batch 2	
Mortality (%)	**Deviation**
15.0	7.1
72.5	3.5
2.5	3.5
67.5	17.7
45.0	7.1
5.0	7.1
3.5	0.0
67.5	3.5
80.0	14.1
80.0	14.1
67.5	3.5
35.0	7.1
57.5	3.5
70.0	7.1
82.5	3.5
65.0	7.1
5.0	7.1
10.0	7.1
50.0	21.2
97.5	3.5
12.5	3.5
57.5	3.5
57.5	3.5
15.0	0.0
62.5	10.6
2.5	3.5
97.5	3.5
7.5	10.6
82.5	10.6
72.5	3.5
70.0	21.2
67.5	10.6
45.0	7.1
67.5	3.5
67.5	17.7
57.5	10.6
89.6	6.6
77.5	3.5
100.0	0.0
75.0	14.1
100.0	0.0

82.5	10.6
5.0	7.1
0.0	0.0
35.0	21.2
2.5	3.5
0.0	0.0
0.0	0.0
0.0	0.0
2.5	3.5
15.0	7.1
27.5	10.6
0.0	0.0
10.0	7.1
0.0	0.0
5.0	7.1
7.5	3.5
2.5	3.5
10.0	7.1
7.5	10.6
15.0	0.0
47.5	10.6
17.5	3.5
40.0	7.1
20.0	7.1
2.5	3.5
2.5	3.5
12.5	3.5
50.0	7.1
10.0	0.0
5.0	0.0
2.5	3.5
2.5	3.5
5.0	7.1
27.5	3.5
0.0	0.0
42.5	17.7
5.0	0.0
32.5	3.5
0.0	0.0
27.5	10.6
5.0	7.1
0.0	0.0
10.0	7.1
10.0	7.1

10.0	7.1
7.5	3.5
17.5	24.7
20.0	7.1

Strain name	**8T5_11**
Number of contigs	29
Genome size	5383205
Number of CDSs	4742
pGV1512-like size	142833
pGV1512-like CDS number	170
Number of genes shared with pGV1512	160
Genome Accession number	NZ_RJJZ01000000.1
pGV1512-like accession number	RJJZ01000012.1

Label in J2-9 (VCR9J2v1_ in MAGE; VCR9J2 in NCBI)
10047
40072
40090
50182
60118
60146
100001
130061
150072
150073
150074
180046
180047
180060
190033
720145
730019
730020
730260
730261
730262
730263
730264
730265
730266
730267
730268
730269
760172
920002
920039
920043
960144
1330033
1350183
1420001
1440001
1570004
1570005
1570006
1600060
1620002
1620025

1630029

Product
Protein of unknown function
Conserved membrane protein of unknown function
Protein of unknown function
Maltoporin
Protein of unknown function
Hypothetical protein
Putative transposase, IS116/IS110/IS902
Conserved protein of unknown function
Putative LysR family transcriptional regulator
Putative exported metal-dependent hydrolase
Exported protein of unknown function
Putative Integral membrane protein, two-component signal transducer
Protein of unknown function
Protein of unknown function
Hypothetical protein
Conserved protein of unknown function
Conserved exported protein of unknown function
Conserved exported protein of unknown function
Putative outer membrane protein
Putative Transcriptional regulator
Putative Phosphotransferase system, fructose-specific IIC component (FruA)
Putative Alpha-mannosidase
Putative sucrose phosphorylase
Putative PTS fructose-specific enzyme IIA component-like protein
Glycerate kinase
Mannose-6-phosphate isomerase
Conserved exported protein of unknown function (R5.7)
Conserved exported protein of unknown function
Conserved protein of unknown function
Hypothetical protein
Conserved protein of unknown function
Conserved hypothetical protein
Conserved hypothetical protein
Conserved membrane protein of unknown function
Protein of unknown function
Transposase
Transposase (fragment)
Putative membrane-fusion protein
Putative N-acetylglucosaminyltransferase
Conserved hypothetical protein
Conserved protein of unknown function
Protein of unknown function
Protein of unknown function

Protein of unknown function

Label (VCR9J2v1_)	Name
30006	argB
30005	argC
720146	hisM
720148	artI
720147	-
720149	artP
750071	***tssM* (*vasK*)**
750073	**-**
750072	**-**
750053	***tssI* (*vgrG*)**
750070	***tssL* (*vasF*)**
750069	***tssK* (*vasE*)**
750068	***tssJ* (*vasD*)**
750067	***fha***
750066	**-**
750065	**-**
750064	**-**
750063	**-**
750062	***tssH* (*vasG*)**
750061	***tssG* (*vasB*)**
750060	***tssF* (*vasA*)**
750059	***tssE* (*vasS*)**
750058	***tssC-2* (*vipB-2*)**
750057	***tssC-1* (*vipB-1*)**
750056	***tssB* (*vipA*)**
750054	***tssA* (*vasJ*)**
750055	***tssD* (*hcp*)**
750086	-

Product	Begin
Acetylglutamate kinase	454077
N-acetyl-gamma-glutamyl-phosphate reductase	453060
Histidine transport system permease protein hisM	2950116
Arginine ABC transporter: substrate binding protein	2951471
ABC transporter: transmembrane protein; Arginine uptake	2950781
Arginine transporter: ATP-binding protein	2952323
Putative type VI secretion protein IcmF/VasK/VtsI	**3615265**
Conserved protein of unknown function	**3619396**
Conserved protein with serine threonine kinase domain	**3618736**
Putative type VI secretion protein VgrG	**3592082**
Putative type VI secretion protein VasF/VtsH/DotU	**3614121**
Putative type VI secretion protein VasE/VtsG/ImpJ	**3612797**
Putative type VI secretion protein VasD-1 (VtsF)	**3612330**
Putative type VI secretion protein VasC/VtsE with forkhead domain (FHA)	**3611302**
Putative type VI secretion protein VtsD	**3610581**
Putative type VI secretion protein VtsC	**3609412**
Putative type VI secretion protein VtsB	**3607172**
Putative type VI secretion protein VtsA D-alanine-D-alanine ligase	**3606015**
Type VI secretion protein VasG (ClpV1)	**3603206**
Putative type VI secretion protein VasB/ImpH	**3602217**
Putative type VI secretion protein VasA/ImpG/TssF	**3600415**
Putative type VI secretion protein VasS	**3600000**
Putative type VI secretion protein, tail sheath-like, (VasRB)	**3598642**
Putative type VI secretion protein, tail sheath-like (VasRA/ImpC)	**3597115**
Putative type VI secretion protein Hcp2/ VasQ/ImpB/VipA	**3596606**
Putative type VI secretion protein VasJ	**3594584**
Putative type VI secretion protein, hemolysin-coregulated protein (Hcp1)	**3595998**
Putative transcriptional regulator (FT1512)	3627769

End	Length	Frame	Normalized average read count
454865	789	3	738
454064	1005	3	1055
2950784	669	-3	176
2952202	732	-1	515
2951467	687	-1	395
2953066	744	-1	608
3618720	**3456**	**1**	**9708**
3620673	**1278**	**1**	**1.49e+4**
3619368	**633**	**1**	**4688**
3594070	**1989**	**-1**	**5560**
3615263	**1143**	**3**	**3046**
3614113	**1317**	**2**	**3996**
3612794	**465**	**3**	**1451**
3612333	**1032**	**1**	**2832**
3611300	**720**	**3**	**2200**
3610584	**1173**	**1**	**3497**
3609415	**2244**	**2**	**6116**
3607169	**1155**	**3**	**5249**
3605818	**2613**	**2**	**1.50e+4**
3603179	**963**	**3**	**7245**
3602217	**1803**	**1**	**8209**
3600422	**423**	**3**	**2482**
3600003	**1362**	**1**	**1.04e+4**
3598593	**1479**	**1**	**2.07e+4**
3597115	**510**	**2**	**1.79e+4**
3595966	**1383**	**2**	**3.45e+4**
3596531	**534**	**3**	**2.74e+4**
3628749	981	1	1.78e+4

Log2 fold change	Adjusted pvalue (FDR)
-2.22	3.42e-44
-2.85	5.73e-73
-2.94	2.92e-55
-2.97	1.19e-66
-3.21	4.93e-72
-3.74	4.51e-98
2.17	**2.11e-51**
2.19	**2.11e-51**
2.24	**7.53e-55**
2.41	**3.37e-62**
2.57	**5.69e-68**
2.62	**1.26e-71**
2.65	**5.23e-65**
2.71	**1.89e-74**
2.84	**3.97e-78**
2.96	**3.09e-88**
3.18	**2.24e-101**
3.71	**2.61e-131**
3.95	**4.18e-142**
4.18	**2.19e-159**
4.53	**6.50e-181**
4.54	**5.92e-168**
4.76	**2.40e-193**
5.59	**1.89e-234**
5.84	**4.07e-253**
5.97	**5.62e-240**
6.25	**9.85e-265**
9.19	0

Strain
Π3813
β3914
GV1975
GV1460
GV2798
GV1438
GV1542
GV2445
GV2702
GV2800
GV2470
GV3196
GV2829
GV2833
A1552
A1552-TnTF1512
GV1495
GV2723
GV1141
GV1484
GV3226
GV3225

Description
lacIQ, thi1, supE44, endA1, recA1, hsdR17, gyrA462, zei298::Tn10 , *DthyA::(erm-pir116)* [Tc^R Erm (F ¯) RP4-2-Tc::Mu ΔdapA ::*(erm-pir116), gyrA462, zei298::Tn10* [Km^R Em^R Tc^R]
8T5_11; *V. crassostreae*
J2-8, *Vibrio sp.* (accession number PRJEB5890)
J2-9, *V. crassostreae* (accession number PRJEB5876)
J2-9 ΔpGV1512
J2-9 ΔPx3 (deletion of the Px3 region within the pGV1512 plasmid)
J2-9 Δtf (deletion of the transcriptional activator *tf* within the pGV1512 plasmid)
J2-9 ΔPx3 + Plac-tf (constitutive expression of *tf* , from a pMRB plasmid)
J2-9 ΔpGV + Plac-tf
J2-9 Δ*paar*
J2-9 Δpaar + Plac-paar (constitutive expression of paar, from a pMRB plasmid)
J2-9 ΔPX3 + Plac-tf
J2-9 ΔPX3 + Plac-gfp (constitutive expression of gfp, from a pMRB plasmid)
V. cholerae O1 El Tor Inaba; WT (#1)
A1552 carrying arabinose-inducible TF on mTn7 transposon (#6624)
J2-9 Δr5-7
J2-9 Δr5-7 ΔpGV1512
J2-9 Δr5-7 + Plac-r5-7 (constitutive expression of *r5.7* , from a pMRB plasmid)
J2-9 Δρ5-7 + Plac-gfp
8T5_11 + Plac-r5-7
8T5_11 + Plac-gfp

Reference
Le Roux et al., 2007
Le Roux et al., 2007
this study
Lemire et al., 2015
Lemire et al., 2015
Bruto et al., 2017
Bruto et al., 2017
This study
This study
This study
This study
This study
This study
This study
Yildiz and Schoolnik, 1998
This study
Lemire et al., 2015
This study
Lemire et al., 2015
Lemire et al., 2015
This study
This study

Plasmid
pSW23T
pSW7848T
pSW7848 ΔPx3
pSW7848 Δtf
pMRB-P_{LAC}-*gfp*
pMRB-P_{LAC}-tf
pSW7848 Δpaar
pMRB-P_{LAC}-paar
pMRB-P_{LAC}*R-5.7*
pSW8742D R5-7
pGP704-TnAraC
pGP704-TnTF1512
pBR-GFP_dsRED_Kan
pTFrep - intergenic region containing putative TF1512 binding site (#6650)
pTFrep - pTFrep deleted for palindromic region (#6685)
pTFrep - pTFrep inversion of palindromic region (#6686)
pTFrep - pTFrep side-specific mutagenesis of palindromic region (#6687)

Description
oriV $_{R6K}$; *oriT* $_{RP4;}$ [Cm^R]
oriV $_{R6K}$; *oriT* $_{RP4}$; *araC*- P_{BAD}*ccdB;* [CmR]
pSW7848T :: ΔPx3
pSW7848T :: ΔPx3-2.5
oriVR6Kg ; oriTRP4; oriVpB1067 $_{;}$ P_{LAC}-*gfp* [CmR]
oriVR6Kg ; oriTRP4; oriVpB1067 P_{LAC}-Px3-2.5 [CmR]
pSW7848T :: Δpaar
oriVR6Kg ; oriTRP4; oriVpB1067 $_{;}$ P_{LAC}-paar [CmR]
oriV $_{R6Kg}$; *oriT* $_{RP4}$; *oriV* $_{pB1067\ ;}$ P_{LAC}*R-5.7* [Cm^R]
pSW8742T :: *D R5-7*
pGP704 with mini-Tn7 carrying araC and PBAD (#5513)
TF cloned behind PBAD promoter of pGP704-TnAraC (#6618)
Promoter-less gfp and dsRed (DsRed.T3[DNT]) reporter genes in aph-carrying plasmid (#1650)
pBR-GFP_dsRED_Kan with intergenic region containing putative TF1512 binding site (#6650)
pBR-GFP_dsRED_Kan with pTFrep deleted for palindromic region (#6685)
pBR-GFP_dsRED_Kan with pTFrep inversion of palindromic region (#6686)
pBR-GFP_dsRED_Kan with pTFrep side-specific mutagenesis of palindromic region (#6687)

Reference
Demarre et al., 2005
Val et al., 2012
Bruto et al., 2018
This study
Le Roux et al., 2011
This study
This study
This study
This study
Lemire et al., 2015
Adams et al., 2019 in press
This study
Lo Scrudato and Blokesch, 2012
This study
This study
This study
This study

Primer
hsp60 For
hsp60 Rev
gyrB For
gyrB Rev
rctB For
rctB Rev
rpoD For
rpoD Rev
pGV1512 *repB* For
pGV1512 *repB* Rev
r5.7 detection For
r5.7 detection Rev
V. crassostreae detection For
V. crassostreae detection Rev
OsHV-1 detection For
OsHV-1 detection Rev
V. aestuarianus detection For
V. aestuarianus detection Rev
FT deletion-1
FT deletion-2
FT deletion-3
FT deletion-4
paar deletion-1
paar deletion-2
paar deletion-3
paar deletion-4
FT complementation For
FT complementation Rev
paar complementation For
paar complementation Rev
PCR VipA For
PCR VipA Rev
PCR FT For
PCR FT Rev
PCR repB For
PCR repB Rev
PCR gyrA For
PCR gyrA Rev
PCR vgrG For
PCR vgrG Rev
Mutagenesis inthe promoter 1
Mutagenesis inthe promoter 2
Mutagenesis inthe promoter 3

Mutagenesis inthe promoter 4
Mutagenesis inthe promoter 5
Mutagenesis inthe promoter 6
Clonage DSred/GFP promoter FT in a MRB plasmid 1
Clonage DSred/GFP promoter FT in a MRB plasmid 2
Clonage DSred/GFP promoter FT in a MRB plasmid 3
Clonage DSred/GFP promoter FT in a MRB plasmid 4

Sequence 5'-3'
GAATTCGAIIIIGCIGGIGAYGGIACIACIAC
CGCGGGATCCYKIYKITCICCRAAICCIGGIGCYTT
GAAGTCATCATGACCGTTCTGCAYGCNGGNGGNAARTTYRA
AGCAGGGTACGGATGTGCGAGCCRTCNACRTCNGCRTCNGYCAT
CAGGAAACAGCTATGACCATHGARTTYACNGAYTTYCARYTNCAY
GATAAACGACGGCCAYTTNCTYTGHATNGGYTCRAAYTCNCCRT
ACGACTGACCCGGTACGCATGTAYATGMGNGARATGGGNACNGT
ATAGAAATAACCAGACGTAAGTTNGCYTCNACCATYTCYTTYTT
CCTCTCTCGACTACACGAAG
CATGCAACTTCATTCCAGGC
CGTATGCCTGAACATAGTTAG
GGGATCTGATGATCACCGAG
AGGTCGCCACTTACTTGCTC
TGCCTTCAGTGAGTTGGGTC
ATTGATGATGTGGATAATCTGTG
GGTAAATACCATTGGTCTTGTTCC
GTATGAAATTTTAACTGACCCACAA
CAATTTCTTTCGAACAACCAC
GTATCGATAAGCTTGATATCGAATTCGGAGGAGTTCATGACCTACA
GCAGTCTCTCAATAACACCGCGCTTCTCTTTTGTGTCCCA
TGGGACACAAAAGAGAAGCGCGGTGTTATTGAGAGACTGC
CCCCCGGGCTGCAGGAATTCGCCATTTCCTATCCAGCGTA
GTATCGATAAGCTTGATATCGAATTCTGCCCATGCCTTACCTGTCC
GGTACGAATTTTGAGTAAGTTATTCTAGGCCTCCAACGGTTGTAG
CTACAACCGTTGGAGGCCTAGAATAACTTACTCAAAATTCGTACC
CCCCCGGGCTGCAGGAATTCTGGTGTCAAGGCCTCGTGGG
GCCCGAATTCATGCTCGACAAAAGAAAACC
GCCCCTCGAGCTAAACCTTACAAACCTGTG
GGGCGGGCCCATGTTACCAGCAGCAAGAGC
GGGCCTCGAGTTAACCGCCAATTAAGACGGTTG
TGTCGGCGTAATTGGCGATT
GAACGGAAGTTCATGCTCAC
GAAATGCTGACAATCGCTGC
CACCACATGCGCCTATTAGT
CACTCTTCCTCTCTCGACTA
CATTAAGCCTACTTTGCGCG
GTTCATACCTAGACTACGCG
ATGCGGGTGGTATTTACCGA
GCCTCAGTTTAGCCTCTATC
CTCAAAGGGTCTTGTGCTTC
CCTTTTCGTCCTAAAAGCCAACCATCTTTATCATCTACCTTTTATTG
CAATAAAAGGTAGATGATAAAGATGGTTGGCTTTTAGGACGAAAAGG
CTTTTCGTCCTAAAAGCCAACtaaatgaggcgtaaatgCATCTTTATCATC

GATGATAAAGATGcatttacgcctcatttaGTTGGCTTTTAGGACGAAAAG
CTTTTCGTCCTAAAAGCCAACcaaaaaaggcgtaaatgCATCTTTATCATC
GATGATAAAGATGcatttacgccttttttgGTTGGCTTTTAGGACGAAAAG
GCCCGAATTCCGTTAAGTGTTCCTGTGTCAC
GCCCCTCGAGCTGCAGACGCGTCG
GCCCCTCGAGTTATTTGTATAGTTCATCCATGCC
GCCCGAATTCCTACAGGAACAGGTGGTGGC

SUPPLEMENTARY DATA

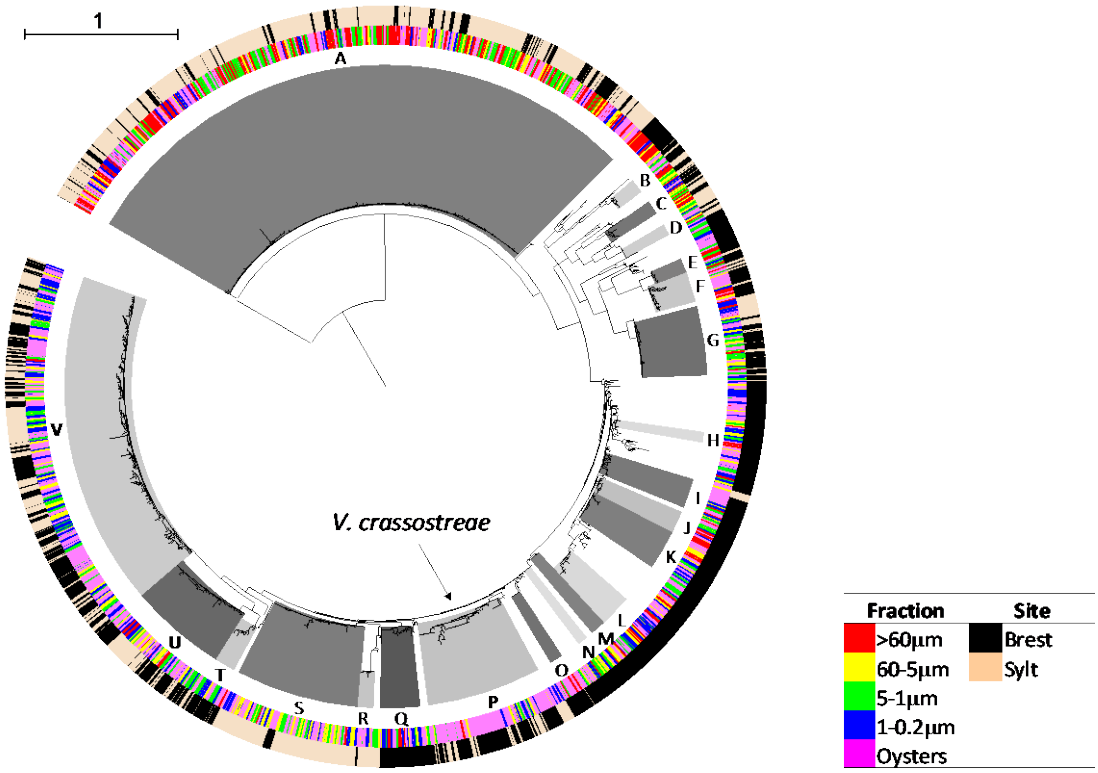

Figure S1 Population structure of *Vibrio* isolates (n=1629) recovered from seawater fractions or oyster tissues from two geographic areas, Brest (France) and Sylt (Germany). Phylogenetic tree (Maximum Likelihood) based on partial *hsp60* sequences. The grey areas correspond to different clades labelled by letters (from A to V) and taxonomically assigned to known *Vibrio* species, *i.e. V. breogani* (A), *V. pacinii* (B), *V. fischeri* (C), *V. alginolyticus* (E, F), *V. jasicida* (G), *V. chagasii* (L), *V. crassostreae* (P) also indicated with a black arrow, *V. kanaloae* (T), *V. cyclitrophicus* (U) and *V. splendidus* (V) or *Vibrio sp. nov* (D, H, I, J, K, M, N, O, Q, R, S). The inner and outer rings indicate the origin of the strain and the site of sampling, respectively, following the colour code given on the right panel.

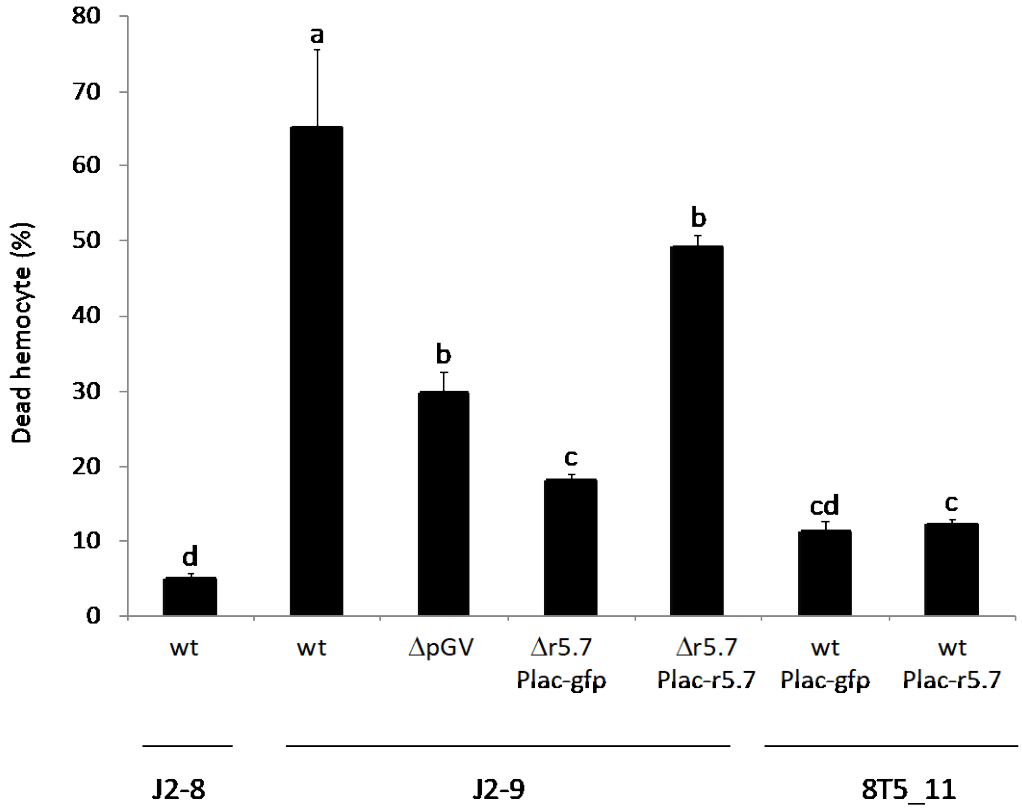

Figure S2 Role of R5-7 in the cytotoxic activity of 8T5-11 strains. The *r5-7* gene or *gfp* as a control were expressed *in trans* from a plasmid in *V. crassostreae* strain 8T5-11 or in a mutant *V. crassostreae* strains J2-9Δ*r5-7*. Cytotoxic activity was assessed by flow cytometry using a double staining procedure after exposition of the cells with bacteria at a ratio of 50 bacteria/hemocyte. As control, hemocytes were either incubated with the wild-type (WT) strain J2-9 or with a non-virulent strain (J2-8). The experiment was performed in duplicate. A single experiment is represented here. Letters indicate significant differences of mortality assessed by simultaneous tests for general linear hypotheses with Tukey contrasts ($P < 0.05$).

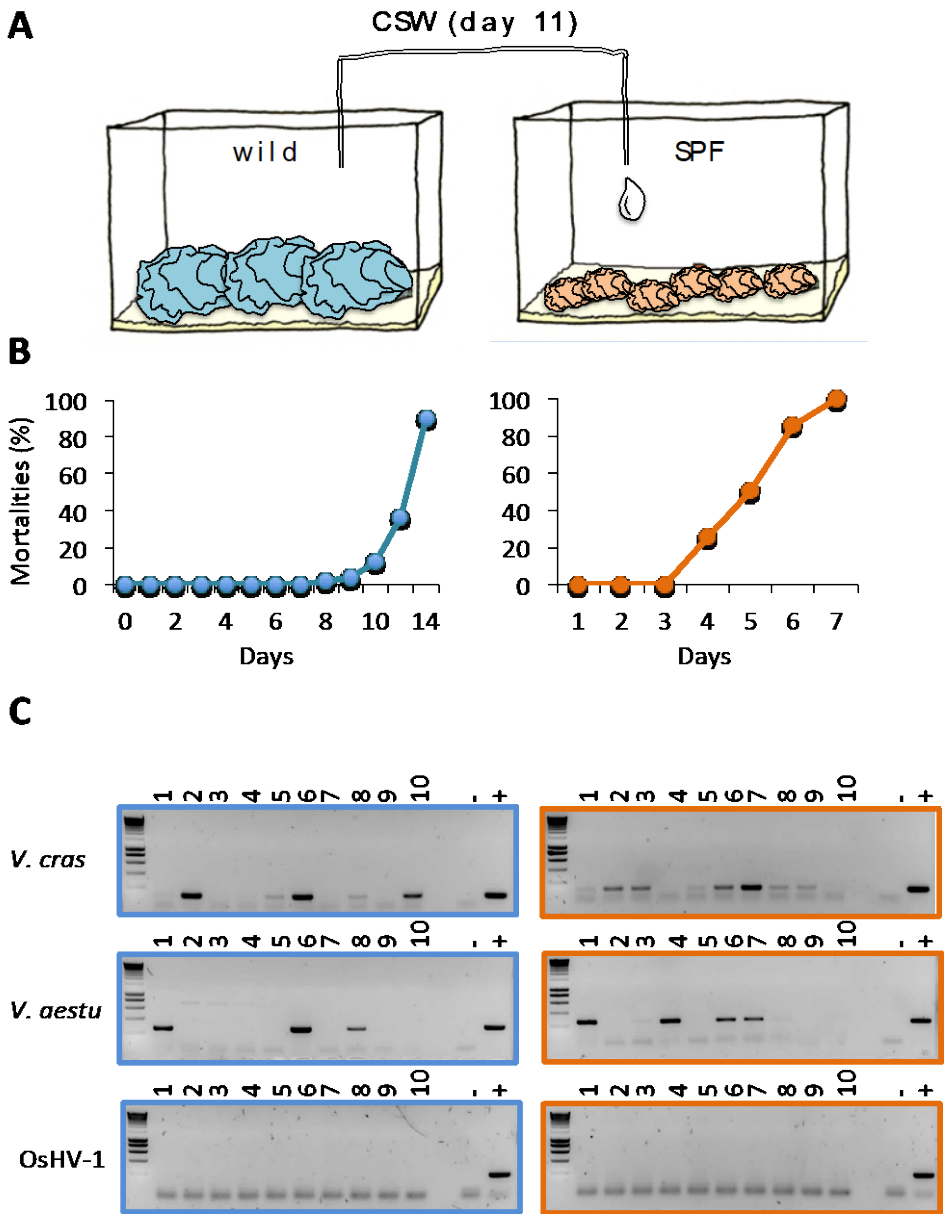

Figure S3 Experimental infection in mesocosm. A. Description of the 'natural' experimental infection. Wild adult oysters (*n* = 50) (animals coloured in blue) sampled in Bay of Brest (seawater temperature of 12°C) were returned to the laboratory and held in a 300-L tank under static conditions with aerated 5-µm-filtered seawater at 21°C. At day 11, three-months-old specific pathogen free oysters (*n* = 20) (animals coloured in orange) were immersed in 1L of

contaminated seawater (CSW) collected from the tank containing the moribund wild oysters or in fresh 5-µm-filtered seawater as a control. **B.** Oyster disease dynamic. Mortality in wild adult oysters (blue line) or in three-months-old juvenile oysters (orange line) was recorded daily for 14 days and 6 days, respectively. Cumulative mortality rates are indicated in % (y axis). **C.** PCR detection of different oyster pathogens. *Vibrio crassostreae, V. aestuarianus* and the Herpes virus OsHV-1 µVar were detected in hemolymph of moribund wild adult oysters (blues boxes) sampled at day 10 (lanes 1 to 4) and day 11 (lanes 5 to 10) or from tissues of moribund three-months-old oysters (orange boxes) exposed to contaminated seawater (CSW) and sampled at day 3 (lanes 1 to 5), day 4 (lanes 6 to 10), day 5 (lanes 11 to 17) and day 6 (18 to 20) post-immersion. The positive (+) and negative (-) signs indicate the positive and negative controls, respectively.

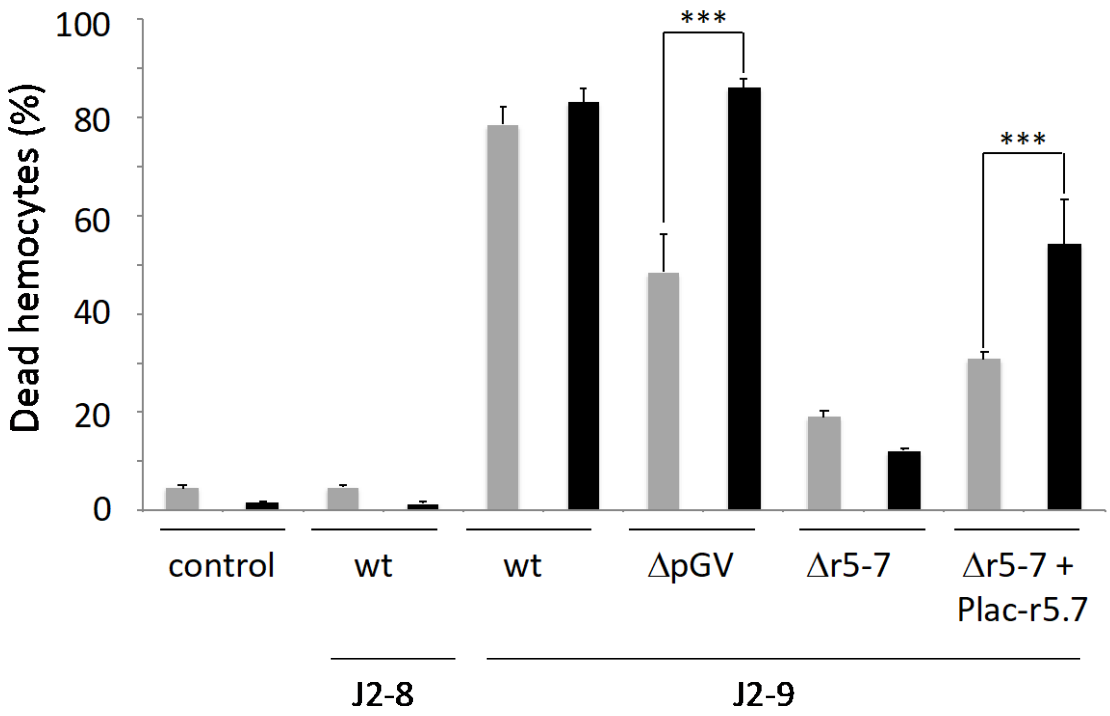

Figure S4 Cell viability assay of oyster hemocytes exposed to different ratios of *V. crassostreae* WT or mutants (Δ). Control hemocytes were incubated without bacteria (control) or with a non-virulent strain (J2-8). Cell viability was evaluated by flow cytometry using a double staining procedure after exposure of the hemocytes to bacteria at a ratio of 10 bacteria/hemocyte (grey bars) or 100 bacteria/hemocyte (black bars) for 6 hours. The assay was performed in triplicate. Asterisks indicate significant differences of mortality assessed by simultaneous tests for general linear hypotheses with Tukey contrasts ($P < 0.05$).

Figure S5 Protein domains found in the transcription factor TF. The protein was annotated with Interproscan. The two domains are represented by colored tubes with numbers indicating the beginning and the end of each domain on the protein. The accession numbers in domain databases (SSF52317 = Superfamily (http://supfam.org/); PF12833 = PFAM (https://pfam.xfam.org/)) are indicated with their putative function beneath.

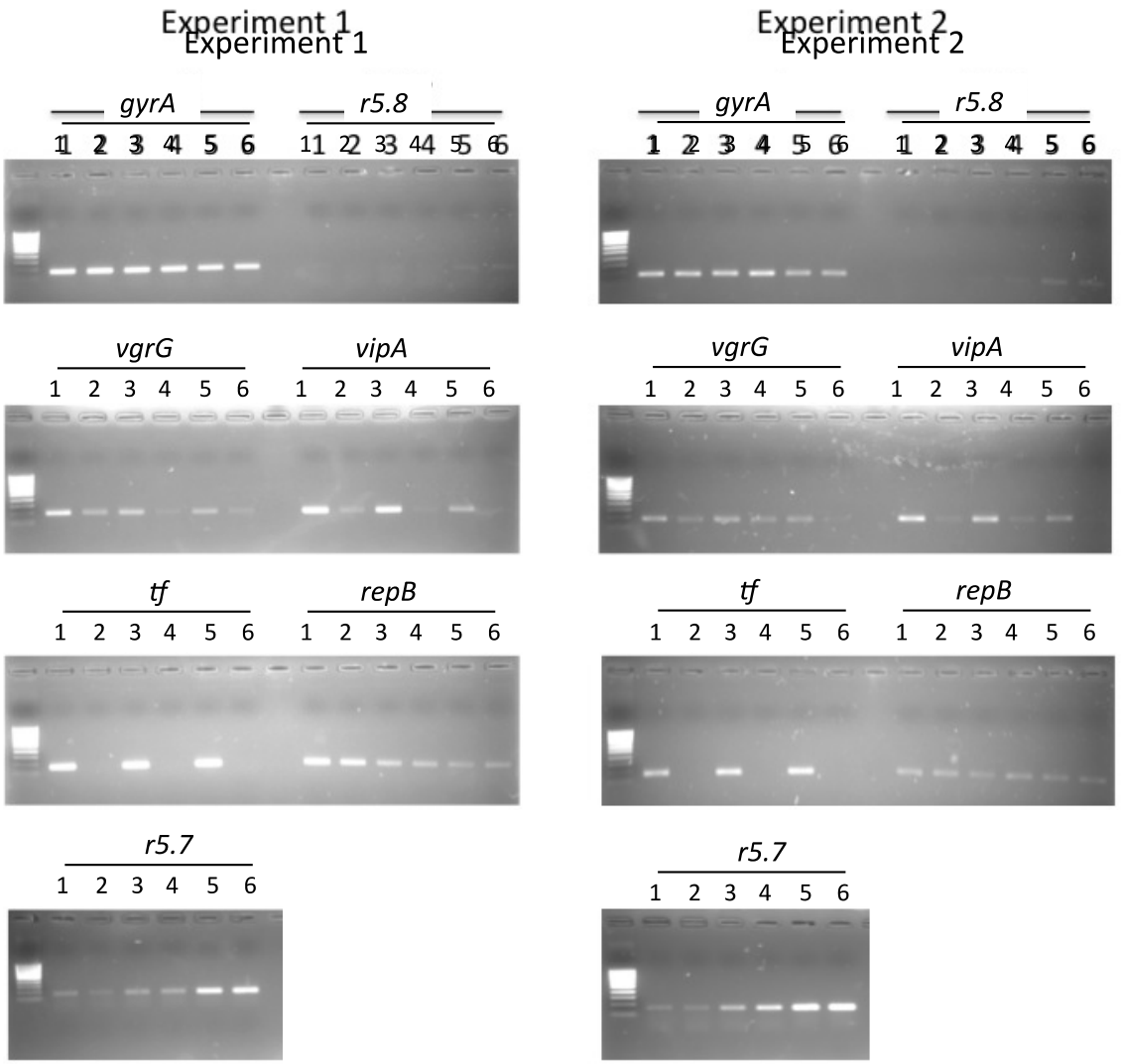

Figure S6 Activation of T6SS genes by the transregulator TF. *V. crassostreae* expressing constitutively the transcriptional factor *tf* (lines 1, 3, 5) or, as a control, the *gfp* (lines 2, 4, 6) were cultivated in marine broth to an optical density of 0.3 (lines 1, 2), 0.6 (lines 3, 4) and 1.0 (lines 5, 6), RNA were extracted, reverse transcribed and used for PCR detection of *gyrA* and *repB* (internal controls), *vgrG* and *vipA* (T6SS), *r5.7* and *r5.8* (chromosomal genes) and the *tf* expressed *in trans* from a plasmid. This experiment was performed twice, as indicated.